CCT-K2: Key Comparison of Capsule-type Standard Platinum Resistance Thermometers from 13.8 K to 273.16 K

A.G. Steele, National Research Council of Canada

ABSTRACT

Calibrated capsule-style standard platinum resistance thermometers were used to compare national realizations of the International Temperature Scale of 1990 (ITS-90) from 13.8033 K, the triple point of equilibrium hydrogen, to 273.16 K, the triple point of water, for seven countries in CIPM Key Comparison CCT-K2. Measurements were made at temperatures close to the eight low temperature defining fixed points of the ITS-90, using a copper comparison block capable of simultaneously holding nine capsules. Two separate measurement runs were performed, allowing two different groups of capsules from each laboratory to be examined. The results are used to determine the degree of equivalence of the independent national realizations of the scale for use in the Mutual Recognition Arrangement Appendix B database. In addition, measurements were also made with the first group of thermometers at approximately eighty temperatures throughout the cryogenic range, which provide information to evaluate some of the so-called scale non-uniqueness issues inherent in the ITS-90 interpolation scheme.

1. INTRODUCTION

In September of 1996, the Comité Consultatif de Thermométrie (CCT) agreed to initiate a series of five international comparisons designed to investigate the degree of equivalence among nations of their independent realizations of the International Temperature Scale of 1990 (ITS-90).[1] These comparisons, covering temperatures from 0.65 K, the lowest point on ITS-90, to 1700 °C, were selected to probe the highest quality measurement capabilities in use around the world, and to test the quality of the scale itself. Subsequent to the CCT meeting, in October of 1999, many of the member countries of the Comité International des Poids et Mesures (CIPM) signed a Mutual Recognition Arrangement (MRA) [2] which put in place a formal scheme for

the signatories to recognize their national standards. The technical basis for this mutual recognition was deemed to be just such international comparisons as were already taking place under the auspices of the CCT. The term "CIPM Key Comparison" was coined to identify these studies, and the CCT comparisons were given designations CCT-K1 to CCT-K5 for use in the Appendices to the MRA. This report covers the work done in CCT-K2: Comparison of Capsule-type Standard Platinum Resistance Thermometers from 13.803 K to 273.16 K.

There were a total of nine national metrology institutes (NMIs) who expressed interest in participating in this study: BNM-INM (France), IMGC (Italy), KRISS (Korea), NIST (United States of America), NMi-VSL (The Netherlands), NPL (United Kingdom), NRC (Canada), PTB (Germany), and VNIIFTRI (Russia). Each laboratory was asked to supply two calibrated capsule-type standard platinum resistance thermometers (CSPRTs) to the pilot laboratory (NRC), where comparison measurements over most of the low temperature range of ITS-90, from the triple point of equilibrium hydrogen (13.8033 K) to the triple point of water (273.16 K) would be carried out. The capsules were delivered to NRC over the period from October 1997 to January 1999.

Two laboratories withdrew from the comparison for technical reasons: NMi-VSL was unable to supply two thermometers with recent realizations of the ITS-90; and measurements made at NRC using the VNIIFTRI thermometers, which were 100 Ω capsules designed and fabricated in Russia, were deemed to be technically compromised due to a lack of communication regarding some special considerations required to obtain the highest accuracy with these devices. A bilateral comparison between NRC and VNIIFTRI will be scheduled following the completion of CCT-K2.

It should be noted that all changes and corrections to the data originally submitted by the participants

were made on the basis of a suggestion by the pilot laboratory that there might be a problem with the values, without indicating either the sign or the magnitude of the observed discrepancy. This is in keeping with the spirit and the letter of the BIPM "Guidelines for Key Comparisons" which were adopted with the signing of the MRA in 1999. The original values and explanations for the changes are included in the text of this document.

This report contains the comparison results in two separate sections: measurements made at temperatures close to the defining calibration fixed-points of the ITS-90, and measurements made throughout the calibration range. For the purposes of Appendix B to the MRA, it is the former data set which is of interest, and results for two groups of calibrated thermometers are shown. The latter data set may be of interest to those considering the non-uniqueness of the ITS-90 scale at the interpolated temperatures in between the fixed points; only one group of thermometers was measured for this purpose.

The goal of this study was to evaluate and summarize the degree of equivalence of the various national realizations of ITS-90, as carried on the calibrated capsule-style thermometers. The comparison was very successful: the results are generally very good, and the thermometers were generally well behaved. In any Key Comparison in thermometry, there is always a danger that the results will be compromised due to the stability of the artifacts being exchanged, especially when thermometers, rather than fixed point cells, are subjected to the rigors of international travel. Careful handling and measurements have yielded a useful set of comparison data in the cryogenic region of the ITS-90.

As defined by the MRA, the degree of equivalence between two measurements (each consisting of a measured value, m_i and its uncertainty, u_i) is expressed by the difference between the measured values ($m_1 - m_2$), and the pair uncertainty of this difference ($u_p = (u_1^2 + u_2^2)^{1/2}$).

A common baseline value for comparisons, against which each individual laboratory's degree of equivalence can be determined, was also introduced in the MRA. It is known as the Key Comparison Reference Value (*KCRV*), and in this study it is calculated as a weighted mean. This experiment involves the use of several calibrated thermometers to make temperature measurements in a common comparison block in a cryostat operating in the pilot laboratory. The measurement differences were obtained directly, using the calibration equations appropriate for the thermometers to determine the block temperature on each laboratory scale. The

uncertainty of the difference involves both the laboratory uncertainty of the thermometer calibrations, and the experimental uncertainty of the comparison measurements themselves. Each of the thermometers has a quoted calibration uncertainty value at each fixed-point temperature, assigned by the participants, denoted $u_L(k=1)$. The measurement uncertainty in the pilot laboratory was determined experimentally, using representative thermometers and standard statistical techniques, denoted $u_{Exp}(k=1)$. Both of these uncertainty components were combined in quadrature to determine the overall comparison uncertainty, denoted $u_C(k=1)$, for each thermometer at each temperature. Thus, the uncertainty in the degree of equivalence will, of necessity, be greater than any individual laboratory's claimed calibration uncertainty. This is a limitation common to all types of comparison, although the "star" topology used here represents perhaps the simplest scheme for evaluating the degree of equivalence of the participants, since no additional uncertainty components are introduced due, for example, to the use of transfer artifacts in a round-robin scheme, or "multiple petals" in other more complicated scenarios. Since all of the various experimental uncertainty components are ascribed to the actual measurements made using the calibrated thermometers, the statistical baseline *KCRV* is taken in this comparison to be an exactly calculated quantity, having no uncertainty. This has the simple advantage that no correlated uncertainty components need be removed when using the degree of equivalence for two laboratories to the *KCRV* to evaluate the laboratory-to-laboratory degree of equivalence. Furthermore, since the *KCRV* temperature differs, however slightly, for the two separate groups of thermometers at each of the comparison points, the lack of an uncertainty in the *KCRV* allows direct comparisons of two thermometers from the same laboratory by inspection.

2. THERMOMETERS: CALIBRATION AND UNCERTAINTY BUDGETS

The low temperature portion of the ITS-90 pertinent to the platinum thermometers used in this comparison defines both calibration point temperatures and deviation equations. The calibration points are the triple points of spin-equilibrated hydrogen, neon, oxygen, argon, mercury, and water, plus two temperatures, near 17.035 K and 20.3 K, which may be realized using either hydrogen vapour pressure measurements, or an interpolating constant volume gas thermometer (ICVGT). The deviation equations are used to relate the temperature-dependence of a

given, real thermometer to the ITS-90 reference function; these are polynomials, the coefficients of which are specific to a given thermometer. The reference function, and its inverse, are also polynomial equations, with universal coefficients defined in the ITS-90. Together, these functions provide the method for continuously relating temperatures to the measured resistance ratio of a calibrated thermometer. The resistance ratio is simply the resistance measured at a given temperature, normalized by taking the ratio with respect to the resistance measured at the triple point of water: $W(T_{90}) = R(T_{90}) / R(273.16 \text{ K})$. The coefficients for the deviation equation are obtained for a given thermometer using each of the measured W values obtained at the calibration fixed points.

Most of the thermometers provided were 25.5 Ω Leeds and Northrup (L&N)-style CSPRTs, some of which were manufactured by YSI; one of the NPL thermometers was manufactured by Tinsley.

The calibration values as supplied by the participants are expressed as resistance ratios, W, at each of the defining fixed points measured in their laboratories. The standard uncertainties at the fixed points are given in mK, also as provided by the participating NMIs. In the text, the combined standard laboratory uncertainties will be labelled u_L, and the tabulated laboratory uncertainty budgets are listed in Appendix A. It should be noted that the protocol for this comparison did not specify the calibration methods to be used, nor did it specify the nature of the uncertainty budgets: these were left as decisions for the participants, and different "common practices" were allowed equally and without prejudice.

There has been some discussion regarding the introduction of some systematic bias into the comparison results due to the different ways in which different laboratories choose to perform their calibrations. In particular, there is some question regarding the choice of where to take the W value on the melting plateau to assign the fixed point temperature. Some laboratories use the 50% melted fraction, some take an average of the values over some range in the middle (between 25% and 90% melted, for example), and some extrapolate the melting curve to 100% melted (the liquidus point). In the case of real samples, where there is a finite slope to the melting plateau, these different schemes give different results. This difference is sometimes accounted for by the addition of an uncertainty component related to the non-zero melting range, or to the choice of the fixed point value. Some argument can be made, however, that a systematic bias still remains due to the application of different techniques. In this Key Comparison, no attempt to

compel the participants to change their practice was made, and no systematic bias which may have been anticipated was observed.

A similar argument surrounds the evaluation of laboratory uncertainty budgets. In many cases, the combined standard uncertainty for any given fixed point value is dominated by a single component, namely that due to chemical impurities and isotopic effects. One common practice for estimating this uncertainty component is to use Raoult's Law, and the first cryoscopic constant, to convert the sample purity into an equivalent temperature uncertainty. Since the majority of chemical impurities are known to depress the phase transition temperature, it may be argued that this uncertainty component should be asymmetric. Similarly, the impact of incomplete spin equilibration at the hydrogen triple point is a "single-sided" error, although this component generally has a much smaller magnitude. The effect of differing isotopic concentrations (particularly important for hydrogen and neon), can be significant, although this can change the transition temperature in either direction, since the variations from the "natural" isotopic ratio can go in either direction. For hydrogen, the concentration of deuterium is usually reduced with respect to the accepted abundance ratio for standard mean ocean water, due to the gas manufacturing and purification process. Some laboratories simply determine the value of these uncertainty components by taking their best scientific estimate; others refine the initial "worst case" value (given by Raoult's Law) by examining several different samples over many years. Some laboratories evaluate this term as a single-sided error, and some consider it to be a symmetric, rectangular distribution. In some cases, the uncertainty due to isotopic concentration effects is left out completely. These are fundamentally different ways of interpreting this component, and give rise to different uncertainty values for something which may have a common origin in the uncertainty budgets prepared by different scientists. Again, it should be emphasized that no prescriptive procedure was given to the participants by the protocol for this comparison experiment, and that all were free to list what they felt best reflected their knowledge of the uncertainty of their calibrations. No attempt to force "harmony" among the various uncertainty budgets has been made during this Key Comparison, although the discussions which have taken place, and the detailed examination of what each NMI is and should be doing with regard to their uncertainty budgets, has certainly brought this issue into the open.

2.1 BNM-INM

Two L&N-style capsules manufactured by YSI were supplied, calibrated for use in the subrange of ITS-90 above 24 K (the triple point of neon). The thermometers were calibrated directly in the BNM-INM fixed points. The $W(Hg)$ values were altered during the comparison from the originally supplied values of $W(1886904, Hg) = 0.844175428$ and $W(1041, Hg) = 0.844172248$. The original calibration measurements at this fixed point were made for both capsules in the same mercury cell, which was later identified as having partially leaked to atmosphere, introducing a corresponding shift in temperature. New measurements performed at BNM-INM in a different Hg cell were used to characterize the temperature shift in the original cell at –2.51mK (±0.05mK). The $W(1886904, Hg)$ listed below was taken from the measurements performed directly in the new cell, while the $W(1041, Hg)$ was corrected via the comparison. The uncertainty in BNM1041 at the mercury point includes a component related to this correction. The corrected values are used throughout the remainder of this report. It should be noted that these (and all other) corrections to the data originally submitted by the participants were made on the basis of a suggestion by the pilot laboratory that there might be a problem with the values, without indicating either the sign or the magnitude of the observed discrepancy. This is in keeping with the spirit and the letter of the BIPM "Guidelines for Key Comparisons" which were adopted with the signing of the MRA.

	1886904		1041	
	W	u_L	W	u_L
H_2	0.001305037	2.08	0.001251856	2.08
17				
20.3				
Ne	0.008581465	0.53	0.008530388	1.40
O_2	0.091853585	0.24	0.09181387	0.23
Ar	0.215974765	0.18	0.215944142	0.20
Hg	0.844165636	0.26	0.844162451	0.27
H_2O	25.584655	0.19	25.572698	0.17

Table 2.1: Calibration data for BNM-INM capsule thermometers.

2.2 IMGC

Two L&N capsules were supplied, calibrated for use in the subrange of ITS-90 above 24 K (the triple point of neon). The thermometers were calibrated directly in the IMGC fixed points. The $W(O_2)$ values

include a known correction to account for the temperature difference between the sample which was used in the calibration run and the best IMGC oxygen cell. The $W(Hg)$ values were altered during the comparison from those originally supplied to properly account for the hydrostatic head correction, which amounted to approximately 1 mK (4.23×10^{-6} in W). In addition, at their request, all of the IMGC low-temperature triple point resistance ratio values were changed from $1/F = 1$ (i.e. liquidus point) values to the measured 50% melt-fraction values obtained from the same melting plateaux. These reductions in the fixed-point W values amounted to temperature-equivalent changes of $-50\,\mu K$ at hydrogen, $-70\,\mu K$ at neon, $-10\,\mu K$ at oxygen, and $-100\,\mu K$ at argon.

	1857277		1860951	
	W	u_L	W	u_L
H_2	0.001191671	0.11	0.001215794	0.11
17				
20.3				
Ne	0.008495882	0.11	0.008503931	0.11
O_2	0.09184464	0.09	0.09181104	0.09
Ar	0.21598525	0.05	0.21594546	0.05
Hg	0.84416905	0.04	0.84415967	0.04
H_2O	25.5496619	0.03	25.5365537	0.03

Table 2.2: Calibration data for IMGC capsule thermometers.

2.3 KRISS

Two L&N-style capsules, manufactured by YSI, were supplied, calibrated for use in the subrange of ITS-90 above 54 K (the triple point of oxygen). The capsules were calibrated directly in the KRISS Ne, O_2, Ar, and H_2O fixed points, and at Hg using a comparison technique. Note that a valid calibration value at the Ne point has been supplied, which is used throughout the paper, although the absence of a calibration point at e-H_2 means that the KRISS realization of the scale stops at 54 K.

	1886906		1043	
	W	u_L	W	u_L
H_2				
17				
20.3				
Ne	0.00852316	0.18	0.00851476	0.18
O_2	0.0918184	0.14	0.0918022	0.14
Ar	0.2159498	0.14	0.2159379	0.14
Hg	0.8441615	0.24	0.8441574	0.24
H_2O	*25.544273*	*0.11*	*25.410822*	*0.11*

Table 2.3: Calibration data for KRISS capsule thermometers.

2.4 NIST

Two L&N capsules were supplied, calibrated for use over the entire low temperature range of ITS-90 above 13.8 K (the triple point of equilibrium hydrogen). Capsule 1774092 was calibrated directly using NIST fixed-point cells for the Ar, Hg, and H_2O triple points, and calibrated by comparison to a reference SPRT using a comparison cryostat at all other fixed-point temperatures. Capsule 1774095 was calibrated directly using the NIST fixed-point cells for the O_2, Ar, Hg, and H_2O triple points, and calibrated by comparison to the same reference thermometer using a comparison cryostat at all other fixed-point temperatures. The reference thermometer, serial number 1004121, was calibrated directly using another cryostat at NIST for cryogenic fixed-point realizations, including e-H_2 vapour pressure realizations of the 17.035 K and 20.27 K points. The W (Hg) values were altered during the comparison from the originally supplied values of W(1774092, Hg) = 0.84415552 and W(1774095, Hg) = 0.844189373. Capsule 1774092 was returned to NIST from NRC for three days during the comparison, and the Hg point was measured again: a difference in the triple point temperature of about 2.5 mK was observed when the original Hg cell was used. This glass Hg cell was investigated for air leaks and for proper immersion, but no such problems were found. Further work at NIST, involving a different Hg cell, confirmed that the original measurements were incorrect (the second cell differed from the original cell by about 2.3 mK). The explanation for the difference involved a small crack in the glass re-entrant well (containing the CSPRT) which was placed into the Hg cell thermowell. The crack allowed alcohol to leak into the region between the two wells, and significantly changed the thermal contact being made with the Hg triple point, in an irreversible fashion. After repairing the leak, new measurements for W(1774092, Hg) were made, and

that value is used throughout the remainder of this report. For 1774095, an archival value for the Hg triple point (measured in 1990, and having a slightly higher uncertainty) was substituted for the originally supplied value, and is used throughout the remainder of the report.

	1774095		1774092	
	W	u_L	W	u_L
H_2	0.001348485	0.12	0.00116574	0.12
17	0.002465625	0.09	0.002273423	0.09
20.3	0.004412745	0.08	0.004215546	0.08
Ne	0.008633776	0.13	0.008433243	0.13
O_2	0.091917108	0.05	0.0917280	0.07
Ar	0.216041	0.05	0.2158770	0.07
Hg	0.844180751	0.11	0.844147275	0.07
H_2O	*25.561811*	*0.08*	*25.527675*	*0.08*

Table 2.4: Calibration data for NIST capsule thermometers. The W(17 K) values were recorded at 17.0357 K, and the W(20.3 K) values at 20.2712 K in a comparison cryostat.

2.5 NPL

Two capsules, one L&N and one Tinsley, were supplied, calibrated for use over the entire low temperature range of ITS-90 above 13.8 K (the triple point of equilibrium hydrogen). Capsule 1728839 was calibrated directly in the NPL fixed points, and using a hydrogen vapour pressure cryostat. The 17 K and 20.3 K calibration points were obtained by adjusting older hydrogen vapour pressure measurements with a small linear correction based on observations of the thermometer drift over time at both the hydrogen and neon triple points. The W(Ar) value was altered during the comparison from the originally supplied value of W(1728839, Ar) = 0.21609660, based on new measurements performed at NPL in the fixed point cell. Capsule 213865 was calibrated by a comparison method against the NPL reference thermometer at temperatures close to the fixed point values. An additional uncertainty component of 0.1 mK, associated with the comparison measurements, is included in the uncertainty budget for 213865. For both of the NPL capsules, the resistance ratios are given at these comparison temperatures: 13.8048 K, 24.5526 K, 54.3669 K, and 233.9998 K. For the argon point, W(1728839, Ar) is given at the usual triple point temperature (83.8058 K), while W(213865, Ar) is listed at 83.8057 K. The impact of changing W(1728839, Ar) as described above was to adjust the reference comparison temperature for 213865 near argon by 0.5 mK.

	213865		1728839	
	W	u_L	W	u_L
H$_2$	0.001237248	0.17	0.001351352	0.14
17	0.002332567	0.22	0.002454326	0.20
20.3	0.004313935	0.22	0.004442955	0.20
Ne	0.008503079	0.20	0.008641441	0.17
O$_2$	0.091812653	0.16	0.091994012	0.12
Ar	0.215914086	0.14	0.216094203	0.09
Hg	0.842877830	0.17	0.842922514	0.14
H$_2$O	25.164672	0.11	25.560733	0.11

Table 2.5: Calibration data for NPL capsule thermometers. The W(17 K) values were recorded at 17.0018 K, and the W(20.3 K) values at 20.3017 K using measurements originally made in a hydrogen vapour-pressure cryostat and subsequently corrected for small observed differences in the hydrogen triple point resistance ratio.

2.6 NRC

One L&N capsule was included, calibrated for use over the entire low temperature range of ITS-90 above 13.8 K (the triple point of equilibrium hydrogen). Capsule 1872174 was calibrated directly in the NRC fixed points, and using a hydrogen vapour pressure cryostat for the 20.3 K point. The hydrogen, neon, and oxygen points were measured in the same apparatus used for the comparison experiments; the argon point was measured in a different cryostat which is also used for measuring long-stem SPRTs; the mercury point was measured in a large glass cell, in an apparatus also used for calibrating long-stem SPRTs. The 17 K point for the NRC scale was obtained during a calibration run at NPL, and is not an independent realization. This thermometer was included in all measurement runs, and may be used to provide a link between the different thermometers from a single NMI which were loaded in the cryostat at different times.

	1872174	
	W	u_L
H$_2$	0.00124008	0.2
17	0.002336324	0.2
20.3	0.004293733	0.2
Ne	0.008516470	0.2
O$_2$	0.091806337	0.2
Ar	0.215944117	0.2
Hg	0.844162509	0.2
H$_2$O	25.499358	0.15

Table 2.6: Calibration data for NRC capsule thermometer. The W(17 K) value was recorded at 17.0018 K (by comparison at NPL), and the W(20.3 K) value at 20.2676 K (in a hydrogen vapour-pressure cryostat at NRC).

2.7 PTB

Two L&N capsules were supplied, calibrated for use over the entire low temperature range of ITS-90 above 13.8 K (the triple point of equilibrium hydrogen). Calibrations were performed directly in the PTB fixed points; the 17 K and 20.3 K calibration points are reported on the basis of independent dielectric constant gas thermometry experiments performed at PTB, and are consistent with the PTB copy of the unadjusted NPL-75 scale. The consequences of the PTB scale values at these two calibration points are discussed more fully in Section 5.2. During the comparison experiments, it was determined that 1842381 had suffered a change in the low temperature residual resistance value, and so it is used throughout the remainder of the report only to provide consistency information on 1842379. The mechanism for determining and correcting for this shift is explained in Section 4.5.

	1842381		1842379	
	W	u_L	W	u_L
H$_2$	0.00118823	0.19	0.00118669	0.19
17	0.00229634	0.28	0.00229467	0.28
20.3	0.00423803	0.28	0.00423625	0.28
Ne	0.0084568	0.18	0.0084553	0.18
O$_2$	0.0917445	0.21	0.0917444	0.21
Ar	0.2158865	0.17	0.2158860	0.17
Hg	0.8441474	0.14	0.8441476	0.14
H$_2$O	25.54599	0.08	25.50632	0.08

Table 2.7: Calibration data for PTB capsule thermometers. The W(17 K) values were recorded at 17.0348 K, and the W(20.3 K) values at 20.2698 K using a dielectric constant gas thermometer.

3. EXPERIMENTAL DETAILS

3.1 Triple Point of Water Measurements

All of the capsules were measured in a triple point of water (TPW) cell at NRC to check for gross problems which might have occurred during transport. In all cases, the capsules were carried by hand from the home country to Canada, with due care being taken to avoid unnecessary shocks. It was not possible to include a residual resistance check, at liquid helium

temperatures, although this would almost certainly have been a more valuable indicator of resistance shifts between measurements due to the low temperature sensitivity of platinum below about 50 K. Figure 3.1 summarizes the results of the "as-received" R_{TPW} measurements. It should be noted that any differences in the national realizations of the Ohm, as carried on the thermometers, will be reflected in the TPW measurements performed at NRC. Each of the error bars represents the standard uncertainty at the TPW assigned by the laboratory, while the dashed lines represent the envelope of the uncertainty for the measurements made at NRC.
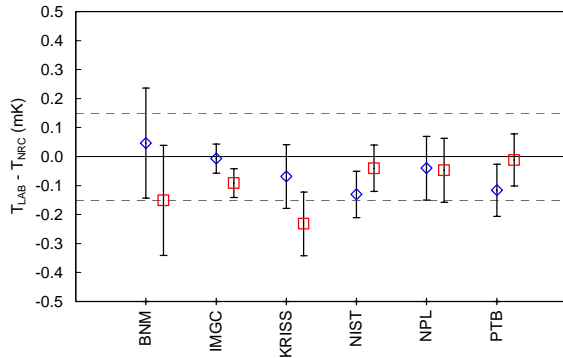
Figure 3.1: As-received triple point of water measurements. The dashed lines represent the standard uncertainty of 0.15 mK for the NRC zero reference; the error bars are the standard uncertainty values ($u_L(k=1)$) supplied by the participants.
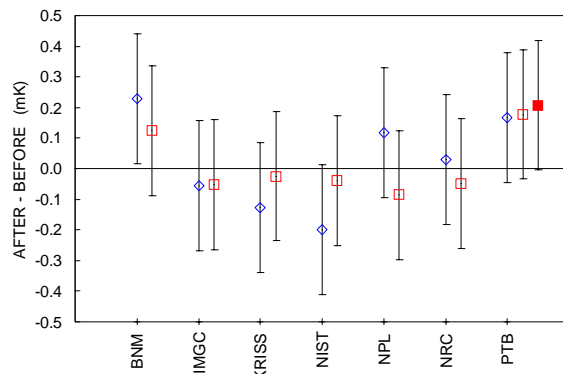
Figure 3.2: Temperature differences for TPW measurements made before and after the measurement runs in the comparison cryostat.

Additional checks of R_{TPW} were performed after the capsules were removed from the cryostat. The equivalent temperature differences (After – Before) are summarized in Figure 3.2. The uncertainty bars, which represent $\sqrt{2}$ times the NRC uncertainty of 0.15 mK, are very conservative, since no account has been made for correlated components common to

both terms in the difference being reported here. In general, the thermometers were observed to be quite stable at the triple point of water after being measured in the cryostat. The R_{TPW} of the PTB 1842379 thermometer, however, was observed to increase systematically over several different measurement runs. An additional uncertainty component, amounting to 0.1 mK, has been propagated to the comparison uncertainties at Hg and Ar for this thermometer to reflect this fact. This is the only additional uncertainty component to be added to account explicitly for thermometer instability observed during the comparison. The remaining thermometers showed no evidence for any large, systematic changes in R_{TPW}: the error bars overlap the zero axis, and there is no systematic increase in resistance as might be expected due to mechanical shock, for example. The good agreement between the two CSPRTs supplied by each participant can be taken as further evidence that no significant instability problems occurred.

3.2   Comparison Cryostat

The CSPRTs were placed in an oxygen-free high-conductivity copper comparison block made for this experiment. The comparison block is cylindrically symmetric, and is capable of holding a single sealed cell fixed point. Eight holes capable of holding an L&N-style capsule were drilled in the annular region surrounding the central sealed cell location. When the smaller diameter Tinsley capsule was being measured, copper shims were used to ensure a good fit. Apiezon-N grease was used to provide good thermal contact between the thermometers and the block. Another CSPRT, from NRC, was placed in the thermowell of the sealed cell as an additional check thermometer, but the data from this capsule are not reported here.

The cryostat was designed and built around a closed-cycle mechanical refrigerator [3], both stages of which could be controlled with an external computer and on-board sensors and heaters. An adiabatic heat shield completely surrounding the comparison block was also actively controlled, and used to balance the temperature of the comparison block at each of the measurement points. One advantage of the mechanical refrigerator is that it was possible to maintain the "bath" temperature seen by the adiabatic shield only slightly below the desired measurement temperature, thus minimizing the heater power required on the adiabatic shield itself. In all of the measurements, this power did not exceed 20 mW, and was typically less than 10 mW. To minimize radiative coupling between the shield and the block

containing the capsules, the inner surface of the shield was lined with a highly reflective film of aluminized mylar. All of the electrical leads were thermally anchored at each stage of the cryostat, with unattached lengths of more than 10 cm left between each of the concentric shells to allow gentle thermal gradients in the wiring, and minimize conduction. The short-circuit electrical resistance of the twisted-pair copper leads for each capsule was approximately 3.5 Ω at room temperature. Outside the cryostat, coaxial cable was used for all connections to the scanner and to the resistance bridge, in order to minimize quadrature errors in the bridge reading.

Measurements were made, using both Pt and RhFe thermometers, to estimate the magnitude of thermal gradients in the comparison block. Separate measurements were made with the thermometers loaded into different positions, both in the block and in the thermowell of the central sealed cell. The temperature differences, averaged for four thermometers and at four different temperatures indicated that the uncertainty due to gradients is approximately 50 μK. Excellent results even at temperatures as high as the triple point of water temperature were obtained, indicating that large thermal gradients were not a significant problem in these comparison experiments.

The effect of thermal conduction through the leads, and through any other direct conduction paths between the comparison block and the temperature-controlled adiabatic shield, was evaluated by taking measurements on the hydrogen triple point plateau and varying the control temperature of the shield. Increasing the shield temperature by 10 mK raised the temperature readings for the thermometers in the block by less than 100 μK. Note that this type of check was made possible due to the thermal pinning effect of the hydrogen phase transition; away from the triple point plateau, increasing the shield temperature by such a large amount would cause the block temperature to ramp steadily upwards. Since the cryostat balance was maintained with shield control at or better than a level of 1 mK, the uncertainty component due to thermal leakage is estimated to be less than 10 μK.

3.3 Resistance Bridge and Measurements

All of the CSPRT resistance ratios were made using an ASL Model F18 AC bridge, with an external ASL Model 148/158 ten-channel, four-terminal scanner used to switch between the thermometers. The 25 Ω standard reference resistor was a Tinsley Model 5685A (S/N 270670), maintained in a temperature-controlled oil bath at 25 °C. The F18 bridge was operated in low frequency (30 Hz) mode, with a gain of 10^4, and at 0.1 Hz bandwidth. Excitation currents were 5 mA for temperatures below 24 K, 2 mA for temperatures between 24 K and 83 K, and 1 mA for temperatures above 83 K. Thermometer self heating was measured at each of the nominal fixed point temperatures, and linearly interpolated for those comparison points in between. The L&N-style capsules all exhibited comparable self-heating, which never exceeded 1 mK. The self-heating for the Tinsley capsule was always greater than for the L&N style capsules, and (prior to changing from 2 mA excitation at 83 K) reached values as high as 1.7 mK. (Note that this large current data point was used only to provide information for the interpolation expressions for the thermometer self-heating at the points in between the fixed points, as discussed in Section 7, below.)

The thermometer resistance ratio values were obtained by taking the average of 10 bridge ratio measurement readings, and then dividing by the average bridge ratio at the triple point of water obtained after the measurement run was completed. The standard error of these W values was typically equivalent to 13 μK. The bridge accuracy specification is 0.2 ppm ratio. No uncertainty component for bridge accuracy is included in the comparison uncertainty budget when reporting temperature differences, since the bridge ratio at each temperature was essentially the same for all of the capsules, and this would represent a completely correlated component, which drops out of the difference calculation. The same holds true for the bridge linearity uncertainty specificiation.

4. COMPARISON EXPERIMENT

All of the measurements were made in round-robin fashion, using the NRC 1872174 CSPRT as a control thermometer to renormalize and correct for any small drift which occurred during the data collection. In practice, this meant first acquiring a bridge ratio value on NRC 1872174; switching the scanner to select the next thermometer; acquiring a ratio value; and finally switching back to the check thermometer before moving to the next capsule. Each thermometer was measured for a period of three minutes, during which time approximately 20 separate resistance ratios were logged to a data file by the computer acquisition software. The first few data points were neglected in order to allow adequate time for the bridge to settle at the new ratio, and so the final value for the bridge ratio was determined by taking the simple arithmetic mean of ten readings. Conversion from bridge ratio to W was made by dividing by the measured triple point of water resistance ratio for the

capsule. The two readings from the check thermometer, taken before and after the capsule reading, were averaged to obtain the equivalent control thermometer ratio; taking this average had the effect of interpolating the control ratio to the same time index as the capsule. This time-equivalent control thermometer reading was then used to determine δW, the difference between the capsule and the control thermometer. Finally, W was determined for the thermometer by adding this δW to the initial control thermometer resistance ratio. In this way, all of the capsule resistance ratios were normalized to "zero time", and the drift was removed from the analysis by linear interpolation.

The data acquisition time for a complete round-robin measurement performed in this fashion was approximately two hours. This includes the time to evaluate the self heating for every thermometer, and for the control thermometer both at the start and end of the cycle; the control thermometer was measured only at the base current setting for each of the drift-correcting measurements performed before and after measuring each of the other capsules. The uncertainty introduced due to the self-heating correction made in this fashion is just the root-sum-square of two averaged bridge readings, and has a value of 19 μK. All of the W values and temperatures reported here are at zero power, with the self-heating effect eliminated.

When the self-heating values were not measured (at temperatures between the ITS-90 fixed point temperatures only), the total time for the measurement cycle was reduced to approximately one hour. For these comparison temperatures, linear interpolation of the self heating was used to perform the correction to zero current. No additional uncertainty due to these interpolated self-heating corrections was included.

4.1   AC Frequency Effects and Uncertainty

Preliminary comparison runs, involving one capsule from each of PTB, NPL, NIST, and NRC, were done to optimize the data collection methodology and evaluate some of the comparison uncertainty components. A capsule from KRISS was also loaded into the cryostat for this work, but since it did not have a supplied full-range calibration, data collected for it are not presented here. Only the listed laboratories were included in this phase of the experiment because these measurements were started before all of the participants had submitted their thermometers.

A serious problem with the original experimental apparatus was found: an apparent frequency dependence of the capsule resistance values manifested itself at very low resistance ratios. The thermometer resistance was observed to change quite dramatically when the AC excitation frequency setting on the bridge was changed from 30 Hz ("low frequency") to 90 Hz ("high frequency"). This effect rendered the original measurements below about 25 K useless, and amounted to a temperature-equivalent difference of more than one millikelvin at 13.8 K. Changing the cryostat wiring from having twisted pairs of (I+, V+) and (I−,V−) as is preferred for use with the DC bridge which had been in routine use in the laboratory, to the more common arrangement (for AC bridges) of using twisted pairs of (I+,I−) and (V+,V−) cured approximately half of the observed frequency dependence. The remainder of the problem was resolved by replacing the original external 2×10 matrix scanner with the ASL 148/158 scanner, rewired internally for use as selecting one of ten thermometer (R_t) channels (as opposed to the more conventional setting with eight R_t and two standard resistor (R_s) channels). Several other scanners were evaluated during this period, without success: all of them caused an observable low temperature frequency dependence on the thermometer resistance. It appears that there is some subtle relationship between the reactance of the external switching scheme and the resistance of CSPRTs which leads to measurement problems in the F18 when the thermometer resistance drops to very low values. Happily, the ASL automatic switch minimized this problem, and the experiments were started once again. A comparison run between 13.8 K and 24.6 K was made to confirm the operation of the new experimental setup. At the lowest temperatures, the frequency dependence of the resistance ratios resulted in apparent temperature differences of not more than 0.2 mK (for the NRC capsule at 13.8 K), and were otherwise well below 0.1 mK. The effect decreased with increasing temperature, and was not discernible at all for temperatures above about 20.3 K. An uncertainty component to account for this effect amounting to 80 μK (only for temperatures below 20.3 K) has been included in the comparison uncertainty budget.

4.2   Key Comparison Reference Value

As mentioned in the Introduction, the data for this comparison are plotted against the weighted average of the individual laboratory values, where the usual normalized inverse of the variances determine the weights. The equation for this scheme is given below, where it should be noted that the u_i values are the

comparison uncertainties $u_c(k=1)$ including the experimental uncertainty $u_{Exp}(k=1)$, and not simply the fixed point uncertainties quoted by each NMI.

$$T_{KCRV} = \sum_{i=1}^{N} T_i / u_i^2 \Big/ \sum_{i=1}^{N} 1 / u_i^2 \quad (1)$$

In the language of the MRA, this weighted average is the so-called Key Comparison Reference Value (*KCRV*), which is used as a notational shorthand for presenting a common baseline against which all laboratory values can be compared. In the case of multiple, independently calibrated thermometers being used to indicate the temperature of a common block, it is reasonable to choose the weighted average of the temperatures, since this is the statistic which is consistent with assuming that all of the laboratories have done a proper job both of assigning temperatures on the ITS-90 and of evaluating their uncertainty budgets. In the absence of other information, this is the statistic that supports the notion that all of the submissions from the individual participants are equally believable. Choosing to use the variances for the individual weights has the advantage that a laboratory with a relatively large uncertainty can still be included in the calculation of the *KCRV*, without unduly influencing its value when the laboratory value turns out to be quite far from the simple arithmetic mean. Since the complete comparison uncertainty (including both the experimental uncertainty as well as the laboratory calibration uncertainty values) is used to determine the weight for each participant, there is no danger that a single laboratory (with a much smaller uncertainty than the other participants) can completely dominate the evaluation of the *KCRV*. This argument is true here since the experimental uncertainty component is comparable to the laboratory uncertainties, but cannot be expected to hold in situations where the comparison uncertainty is significantly smaller than the laboratory uncertainty. For this experiment, the weighted average of the independent values is a reasonable choice for a Key Comparison Reference Value.

4.3 Initial Comparison Results

The group of capsules initially loaded into the cryostat are listed in Table 4.1. Subsequent to the earliest measurements which were affected by the AC frequency dependence problem discussed in Section 4.1, a series of low temperature comparison measurements was made starting at the hydrogen point and proceeding up to the neon point. This experiment had two goals: to further characterize the measurement system; to obtain some information about the comparability of the calibrated

thermometers at temperatures in between the defining fixed points of the ITS-90.

Laboratory	Serial Number	Position
PTB	1842379	1
NPL	1728839	2
NIST	1774092	4
NRC	1872174	8

Table 4.1: Four capsules were loaded into the comparison cryostat for the preliminary measurement run.

The results for this low temperature comparison run of four capsules, are shown in Figure 4.1. This data set includes measurements made at a total of 52 temperatures, including the calibration fixed points. The scales are seen to be in reasonable agreement with each other, with differences in this temperature range not exceeding about 0.6 mK. The smoothness of the individual curves is expected from the interpolation formula, and indicates that the data are of reasonably high quality. The error bars, shown only at the fixed points, are standard errors, including both the calibration and experimental uncertainty components.
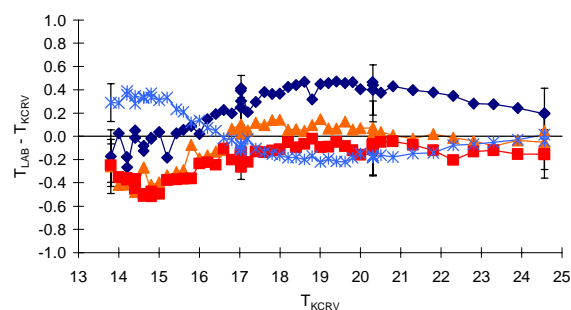
Figure 4.1 – Temperature deviations for four capsule thermometers at the low end of the platinum range in ITS-90. The symbol key for this graph is: triangle = NRC 1872174; diamond = PTB 1842379; square = NPL 1728839; star = NIST 1774092.

The measurement repeatability at substantially the same block temperature was tested by making separate, complete round-robin measurements without significantly changing the control setpoint for the adiabatic shield. Short term and long term repeatability were assessed by performing the repeat measurements either immediately after the first set, by waiting one hour after slightly changing the cryostat balance point, or by leaving the cryostat overnight and doing the repeat measurement the next morning. In Figure 4.1, there are three points at 17 K, three points at 20.3 K, and two points at 24.55 K for

each of the four thermometers. The graph shown below in Figure 4.2 summarizes this reproducibility check, for measurements made close to three of the ITS-90 calibration fixed point temperatures. Taking the standard deviation of the differences for each of the four thermometers at each of the three temperatures yields twelve separate estimates of the measurement reproducibility. The average of these values is 32 μK, which is used as the "repeatability component" in the comparison uncertainty budget.

The ITS-90 reference function, and the propagation of fixed point uncertainties, together give perfectly smooth behaviour for interpolated temperatures between the fixed points. The overall "smoothness" of the individual curves in Figure 4.1 is indicative of the quality of the experimental results; for most of the capsules, over most of the range, the experimental limit on this smoothness is estimated to be 50 μK. This can be thought of as an additional experimental uncertainty component for the comparison, evaluated as a Type B component. Although the 'smoothness' and 'repeatability' components may be somewhat correlated, no significant double counting occurs in the total experimental uncertainty budget when both are included.
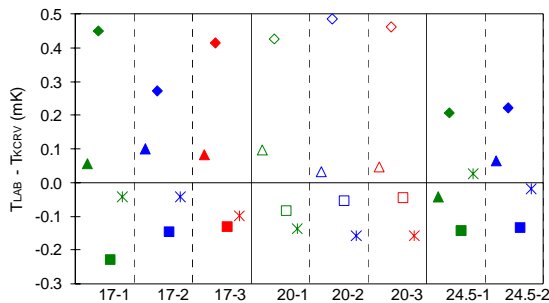
Figure 4.2: Repeatability check near three low temperature ITS-90 calibration points: three repeat measurements at 17 K, three repeats at 20.3 K, and two repeats at 24.5 K. The same symbols are used as in Figure 4.1: triangle = NRC 1872174; diamond = PTB 1842379; square = NPL 1728839; star = NIST 1774092. The average experimental reproducibility from this set of twelve independent evaluations is 32 μK.

To justify this statement, a typical case is examined. It may be noted that leaving the 'smoothness' component entirely out of the combined experimental standard uncertainty calculation lowers the $T>20.3$ K value from 84 μK to 67 μK (i.e. by about 20%); the $T<20.3$ K value would

be reduced from 116 μK to 105 μK (i.e. by about 10%). The final comparison uncertainty, however, is determined by adding the experimental uncertainty and the laboratory calibration uncertainty terms in quadrature. Taking a typical value for $u_L(k=1)$ of 150 μK, the impact of ignoring the term corresponding to 'smoothness' from the experimental uncertainty budget is very small: for $T<20.3$ K, the reduction is about 4% (190 μK to 183 μK), while for $T>20.3$ K, it is about 5% (172 μK to 164 μK).

4.4 Experimental Uncertainty Budget

The experimental measurement uncertainty budget including the components discussed above is summarized in Table 4.2. The combined standard errors used throughout the remainder of this report are: $u_{Exp}(k=1; T<20.3$ K$) = 0.12$ mK and $u_{Exp}(k=1; T>20.3$ K$) = 0.09$ mK. These values are summed in quadrature with the laboratory uncertainty statements at each of the fixed point temperatures to obtain the complete comparison standard errors used in the tables and graphs.

Experimental Uncertainty Components	Value (μK)
thermal gradients in block	50
thermal leakage to block	10
bridge reading (average)	13
self-heating correction	19
drift correction	20
frequency effect (average)	80 ($T< 20.3$ K)
repeatability at single T	32
"smoothness" versus T	50

Combined standard uncertainty ($T<20.3$ K)	$u_{Exp}(k=1) = 116$
Combined standard uncertainty ($T>20.3$ K)	$u_{Exp}(k=1) = 84$

Table 4.2: Experimental measurement uncertainty budget. This component, $u_{Exp}(k=1)$, is combined in quadrature with the laboratory calibration uncertainty, $u_L(k=1)$.

As a final check on the experimental measurement uncertainty, the data for two thermometers measured in two comparison runs was compared, after all of the measurements had been completed. The consistency of the differences between the temperatures indicated on the two CSPRTs may be used to evaluate the confidence in the uncertainty estimate in Table 4.2. First, the temperature difference at each of the comparison temperatures was calculated for seven comparison

points in each of two runs, giving a total of fourteen values $\Delta T_{1,i}$ and $\Delta T_{2,i}$; next, the second-run difference, $\Delta T_{2,i}$, was subtracted from the first-run difference, $\Delta T_{1,i}$, giving seven differences $\Delta T_{1-2,i}$; finally, the standard deviation of these seven values was calculated, in order to estimate uncertainty due to scatter in the comparison results. It should be noted that this procedure does not involve the laboratory uncertainty in any way. The standard deviation was determined to be $\sigma(\Delta T_{1-2,i}) = 0.11$ mK, which is entirely consistent with $u_{Exp}(k=1)$ as evaluated here. This consistency evaluation is detailed in Section 5.9.

4.5 Comparison Uncertainty and Correlations

It is worth detailing the methods used to combine the various uncertainty components used in this work, and indicating possible sources of correlation in the comparison uncertainty values used throughout the text, as well as in the Figures and Tables which follow. As has been discussed above in Section 2, each of the participants submitted a laboratory calibration uncertainty for their thermometers; this is represented by $u_L(k=1)$. Also, as itemized in Section 4.3, the experimental uncertainty on the measurements made in the comparison cryostat has been estimated at the pilot laboratory; this is represented by $u_{Exp}(k=1)$. The combined standard uncertainty for the comparison is then taken to be the root-sum-square of these two components; this is represented by $u_C(k=1)$, and is evaluated according to Equation 2.

$$u_C = \sqrt{u_L^2 + u_{Exp}^2}$$ (2)

In the equivalence analysis which follows in Sections 5 and 6, the measured temperature values as indicated on each of the thermometers are combined to provide a common reference temperature according to Equation 1 from Section 4.2: a weighted average of the independent temperature scales. This so-called Key Comparison Reference Value (*KCRV*) is taken to be the average of the independent measurements, weighted by the reciprocal of the square of the comparison uncertainty (u_C).

When reporting the laboratory-to-laboratory degree of equivalence, in the full-bilateral summary matrix format of Appendix B for example, the pair uncertainty has been taken as the simple combined standard uncertainty using the comparison uncertainty values for each laboratory.

$$u_p = \sqrt{u_{C1}^2 + u_{C2}^2}$$ (3a)

This analysis is based on the assumption that the experimental uncertainty component, u_{Exp}, which is common to both u_{C1} and u_{C2}, is completely uncorrelated. If experiments could be designed to illustrate, for example, that the u_{Exp} terms were completely correlated, such as might be imagined for a constant bias effect introduced through the thermal gradient term, or through a quadrature term identical for all thermometers, then the u_{Exp} terms would drop out of Equation 3a, and the pair uncertainty expression would involve only the laboratory calibration uncertainty terms as shown in Equation 3b.

$$u_p = \sqrt{u_{L1}^2 + u_{L2}^2}$$ (3b)

Given the nature of the terms included in u_{Exp}, it seems reasonable and conservative to assume that the two instances are uncorrelated. Furthermore, the impact of assuming a fully correlated experimental uncertainty on u_p is quite small: given $u_{L1} = 0.20$ mK, $u_{L2} = 0.15$ mK and taking $u_{Exp} = 0.09$ mK, Equation 3a gives $u_p = 0.28$ mK, while Equation 3b gives $u_p = 0.25$ mK; the difference is only about 30 μK, or some 11% of the uncertainty value. This would be the maximum change in the pair uncertainty if all but the quadrature components were determined to be fully correlated. In practice, this shows that the conservative approach – assuming that all of the experimental uncertainty components are uncorrelated among the thermometers being compared – has little or no impact on the analysis which follows.

4.6 Residual Resistance Correction

The low temperature values for PTB 1842381 in the Group A comparison appeared to be inconsistent with the preliminary results determined using PTB 1842379, and discussed above in Section 4.3; in particular, there was an apparent deviation of more than 1 mK for this capsule at the hydrogen triple point, when the preliminary data indicated very good agreement between, for example, the PTB and NPL scales at this temperature. The temperature dependence of the experimental difference indicated that capsule PTB 1842381 had suffered a change in residual resistance, either during transit or during the comparison experiments, and therefore was no longer representative of the PTB realization of the ITS-90. During the Group B comparison, therefore, both of the PTB capsules were loaded into the comparison block. The direct comparison made during this experimental run confirmed the residual resistance-shift hypothesis, and suggested a solution. A correction to the resistance ratio, $W(1842381)$, to account for the change in the low temperature residual resistance, δR, was performed for PTB

1842381. The value of $\delta R = -6.61\,\mu\Omega$ was determined using the following simple model equation, and matching the temperatures for the two PTB capsules at the triple point of hydrogen.

$$W' = \frac{(R(T) + \delta R)}{(R(273.16\text{K}) + \delta R)} \qquad (4)$$

This correction, determined during the comparison measurements, is applied throughout this paper to PTB 1842381, and therefore the results for this capsule should be viewed not as a simple representation of the PTB realization of ITS-90; there is an additional uncertainty component which propagates to higher temperatures via the equation above which would not appear in a normal PTB calibration. Taking the partial derivative of Equation 4 with respect to δR gives the sensitivity coefficient for this correction.

$$\frac{\partial W'}{\partial(\delta R)} = \frac{(R(273.16\text{K}) - R(T))}{(R(273.16\text{K}) + \delta R)^2} \qquad (5)$$

The uncertainty in δR may be estimated from the comparison uncertainty in temperature (0.12 mK) and the platinum resistance temperature sensitivity at 13.8 K (6.1 $\mu\Omega$/mK), leading to a value of $u(\delta R) = 0.7\,\mu\Omega$. Using this residual resistance uncertainty along with the sensitivity coefficients obtained from Equation 5, and the sensitivity coefficient for converting uncertainty in W to equivalent temperature from the ITS-90 reference function, the individual temperature uncertainties due to $u(\delta R)$ can be calculated at all higher temperatures. This procedure leads to additional uncertainty components of 60 μK at 17 K, 36 μK at 20.3 K, 22 μK at 24.5 K, and 6 μK at 54.4 K; for temperatures above the oxygen triple point, the contribution may be completely ignored, since it is less than 2 μK, and vanishes altogether at the triple point of water. These additional uncertainty values associated with making the residual resistance correction have been properly incorporated in all subsequent calculations for PTB 1842381.

Nevertheless, both PTB thermometers can be compared to check consistency. The data for this thermometer, once corrected, are seen to be in close agreement with the PTB scale, as carried by PTB 1842379. It should be noted that the correction δR was determined using only the 13.8 K comparison data from the Group B measurement run; there are no other "fitting parameters" for the higher temperature comparison points, and so the two PTB thermometers remain virtually independent. The good agreement between the two at all higher temperatures indicates that the calibration carried by the PTB 1842379

capsule has remained stable during this comparison experiment. The very good agreement observed between the two measurements at 13.8 K with PTB 1842381 indicates that this thermometer remained quite stable in the comparison cryostat.

As a visual reminder that the residual resistance correction has been added to PTB 1842381, this thermometer is labelled with an asterisk ('*') in the Figures and Tables which follow in Sections 5 and 6.

5. COMPARISON RESULTS NEAR THE ITS-90 FIXED POINT TEMPERATURES

Following the initial measurements described in Section 4, one capsule from every participant was placed in the cryostat for a complete comparison run at temperatures close to the ITS-90 calibration temperatures. Subsequently, a second measurement run was performed with the other capsule from each NMI loaded into the cryostat. The same thermometer from NRC was used in both of these comparison runs, and therefore provides a direct link between the Group A and Group B results. It must be emphasized that the temperature of the comparison block is given by every thermometer, reflecting the different national realizations of ITS-90. Table 5.1 lists the capsules that were loaded simultaneously in each of the two Groups, along with their positions in the comparison block. The thermowell positions were numbered sequentially around the cylindrical comparison block, and position 1 is adjacent to position 8. The two capsules from each laboratory were placed in the same positions in both of the measurement runs for simplicity in bookkeeping, although this strategy may be susceptible to small systematic effects due, for example, to thermal gradients in the block, or to differences in the wiring among the different channels. Neither of these effects is expected to be significant, however, and the comparison results tend to support this.

Group A CSPRTs		
NMI	*Serial Number*	*Position*
PTB*	1842381	1
NPL	213865	2
KRISS	1886906	3
NIST	1774095	4
BNM	1886904	6
IMGC	1857277	7
NRC	1872174	8

Group B CSPRTs		
NMI	*Serial Number*	*Position*
PTB	1842379	1

NPL	1728839	2
KRISS	1043	3
NIST	1774092	4
PTB*	1842381	5
BNM	1041	6
IMGC	1860951	7
NRC	1872174	8

Table 5.1: Capsules from each NMI were loaded into the comparison cryostat for each measurement run in two separate Groups.

Throughout the remainder of this Section, the comparison values near each of the ITS-90 low temperature fixed points are reported. The tables list the observed resistance ratio (W) values for each of the thermometers, along with the deviations from the *KCRV* temperature, and the comparison uncertainty. The *KCRV* temperature is evaluated according to Equation 1, as discussed in Section 4.2. The comparison uncertainty, u_C, is evaluated according to Equation 2, as discussed in Section 4.4. There is no additional uncertainty associated with the *KCRV* itself.

Two tables are presented at each comparison point: one for the Group A thermometers, and one for the Group B thermometers. Both data sets are shown in the corresponding figure: the Group A data are shown as diamonds, and the Group B data are shown as squares. All of the uncertainty values represent standard uncertainties. In Appendix B of this Report, the full bilateral equivalence matrix is provided for each of these fixed point comparison data sets. The data presented in Appendix B are the basis for the entry for CCT-K2 in the MRA Appendix B database, although the format used here is slightly different. For this experiment, the MRA database entry is reported with a coverage factor $k=2$ which represents a confidence level of 95% when the underlying probability density function is assumed to be Gaussian.

The zero of each plot is placed at the *KCRV*, and the differences $T_{LAB} - T_{KCRV}$ are chosen such that a positive value is representative of a thermometer which indicates a hotter-than-average temperature (as is the convention for this round of Key Comparisons). On the other hand, this sign convention for the observed temperature deviations means that a positive value indicates a *colder* fixed point value. The reader is reminded of this fact to forestall confusion when drawing conclusions about the relative values of the calibration fixed points used in each laboratory.

5.1 Near e-H₂ TP

The cryostat was balanced for comparison near the triple point of spin-equilibrated hydrogen: the two *KCRV* temperatures were within 0.5 mK of 13.8033 K. Both BNM and IMGC have valid calibration data points at this temperature as required to realize the ITS-90 down to the Ne triple point temperature.

The scatter of the temperature differences, taken as a simple standard deviation of the *T-KCRV* values for both Group A and B thermometers (excluding the BNM-INM data, and the PTB 1842381 value) is 0.28 mK.

Lab	S/N	W	*T-KCRV*	u_C
BNM	1886904	0.001 304 310	-2.71	2.08
IMGC	1857277	0.001 191 521	-0.32	0.16
NIST	1774095	0.001 348 515	0.42	0.17
NPL	213865	0.001 236 821	0.07	0.21
NRC	1872174	0.001 239 948	-0.26	0.23
PTB*	1842381	0.001 188 456	0.16	0.26
BNM	1041	0.001 251 264	-2.60	2.08
IMGC	1860951	0.001 215 793	-0.17	0.16
NIST	1774092	0.001 165 881	0.42	0.17
NPL	1728839	0.001 351 002	-0.05	0.18
NRC	1872174	0.001 240 055	-0.27	0.23
PTB	1842379	0.001 186 724	-0.02	0.22
PTB*	1842381	0.001 188 523	-0.02	0.26

Table 5.1: Comparison data near the triple point of hydrogen.
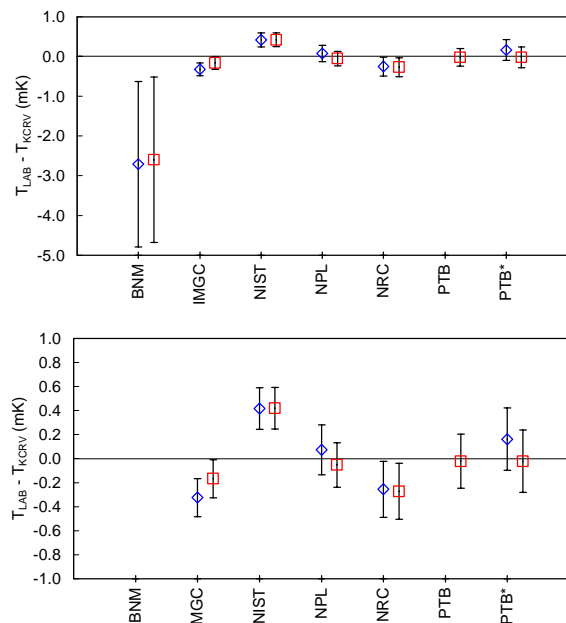
Figure 5.1: The comparison near 13.8033 K, the triple point of spin-equilibrated hydrogen. An expanded-scale graph (excluding the BNM points) is also shown.

5.2   Near 17 K: 33.3 kPa e-H_2 BP or ICVGT

The comparison near 17 K was made by balancing the cryostat to within 0.5 mK of 17.035 K. The NRC calibration point is included in this analysis, although it is not an independent realization but rather was assigned during previous comparison measurements made at NPL. For this reason, the NRC value is not used to calculate the KCRV at this temperature.

The calibration point near 17 K may be realized according to the definition of the ITS-90 in two separate ways: as a vapour pressure measurement of equilibrium hydrogen, or using an interpolating constant volume gas thermometer (ICVGT) which has been calibrated between 3 and 5 K, using He vapour-pressure thermometry, and at the triple points of e-H_2 and Ne. The NIST and NPL realizations were determined via hydrogen vapour pressure measurements; the NRC value was assigned by comparison measurements made at NPL.

At PTB, an interpolating dielectric constant gas thermometer was used to as an approximation to the ITS-90 to realize the 17 K and 20.3 K calibration points. This strategy is similar to using an interpolating constant volume gas thermometer, in that the apparatus is calibrated for interpolation at three temperatures. In this case, PTB used 4.8 K, 13.8 K, and 24.6 K, since these are very close to the

values recommended in the ITS-90 for calibrating the ICVGT.

Additional PTB data at this temperature, and at 20.3 K, are available from an unadjusted copy of NPL-75, which is a widely-used low temperature scale based on thermodynamic temperature measurements. Using this alternate calibration technique leads to CSPRT W values at 17 K and 20.3 K which are lower by temperature equivalents of 0.21 mK and 0.19 mK, respectively (as compared to the DCGT values which are included in Table 2.7). Thus, for CSPRT 1842379, the deviations from the KCRV temperatures would be increased accordingly. These points have standard laboratory uncertainties of 0.17 mK, and the combined comparison uncertainties amount to 0.21 mK. A data point, with symbol '×', has been added to Figure 5.2 to indicate this alternative approach. This data point has a value $T-KCRV = 0.43$ mK, with a combined comparison uncertainty of 0.21 mK.

It is interesting to note that there appears to be an experimental discrepancy between the 17 K comparison measurements for the thermometers calibrated using either the hydrogen vapour pressure realization of ITS-90 (NIST 1774092 and NPL 1728839) or dielectric constant gas thermometry (PTB 1842379) and the NPL-75 scale (the alternate PTB 1842379 calibration).

There has been some speculation about non-uniqueness in the ITS-90 itself at 17 K and 20.3 K, and Meyer et al. have recently made measurements which suggest that the non-uniqueness can be as large as 0.5 mK at 17 K.[4] Since none of the thermometers used in this Key Comparison carry ITS-90 assignments made by ICVGT, however, no information concerning this potential source of non-uniqueness exists here.

It has also been pointed out that NPL-75 and ITS-90 disagree by about 0.6 mK at 13.8 K and by about 0.1 mK at 24.5 K, with NPL-75 being higher.[5] A simple linear interpolation predicts that $T_{90} = T_{75} - 0.45$ mK at 17 K, and $T_{90} = T_{75} - 0.30$ mK at 20.3 K. The data described here (and in Section 5.3, where the 20.3 K comparison data are summarized) are not inconsistent with this scale discrepancy.

Further information concerning differences between different scale realization strategies might be available within the context of the CCT-K1 Key Comparison of RhFe Thermometers in the temperature range below 24.5 K.

The scatter of the temperature differences, taken as a simple standard deviation of the T-KCRV values for both Group A and B thermometers (excluding the PTB 1842381 data) is 0.11 mK.

Lab	S/N	W	$T\text{-}KCRV$	u_C
NIST	1774095	0.002 465 229	-0.01	0.15
NPL	213865	0.002 347 708	0.06	0.25
NRC	1872174	0.002 351 472	0.05	0.23
PTB*	1842381	0.002 296 609	-0.04	0.31
NIST	1774092	0.002 272 922	0.01	0.15
NPL	1728839	0.002469357	-0.09	0.23
NRC	1872174	0.002 351 418	0.18	0.23
PTB	1842379	0.002 294 680	0.21	0.30
PTB*	1842381	0.002 296 574	0.13	0.31

Table 5.2: Comparison data near the 17.035 K calibration temperature.
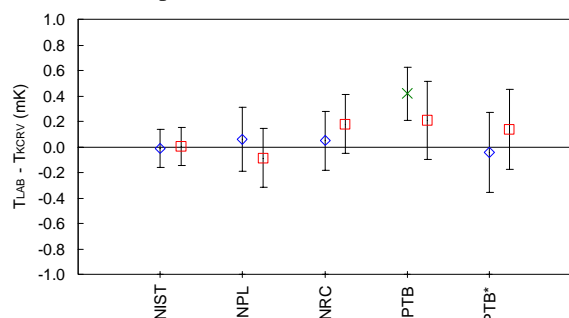
Figure 5.2: The comparison near the 17.035 K calibration temperature.

5.3   Near 20.3 K: 101.3 kPa e-H_2 BP or ICVGT

As is the case with the 17 K point, calibration near 20.3 K may be performed using hydrogen vapour pressure measurements, or using an interpolating constant volume gas thermometer. For the comparison measurements, the cryostat was balanced within 0.5 mK of 20.270 K.

The NRC assignment for this temperature is not tied to the earlier calibration by comparison done at NPL; rather it was obtained in a hydrogen vapour cryostat, and is therefore included in the calculation of the *KCRV* temperature. Similarly, the NPL and NIST realizations are based on hydrogen vapour pressure measurements. The PTB value, as for the 17 K point, is reported using dielectric constant gas thermometry as an approximation to ITS-90.

An extra point, representing an alternative PTB calibration of CSPRT 1842379 at 20.3 K based on a copy of the NPL-75 temperature scale has been added to Figure 5.3, with symbol '×'. This data point has a value $T-KCRV = 0.60$ mK, with a combined comparison uncertainty of 0.21 mK. Section 5.2 contains a detailed description and explanation for the inclusion of this additional information.

The scatter of the temperature differences, taken as a simple standard deviation of the *T-KCRV* values for both Group A and B thermometers (excluding the PTB 1842381 data) is 0.17 mK.

Lab	S/N	W	$T\text{-}KCRV$	u_C
NIST	1774095	0.004 412 085	0.00	0.14
NPL	213865	0.004 290 209	-0.06	0.25
NRC	1872174	0.004 295 846	0.06	0.23
PTB*	1842381	0.004 238 664	0.00	0.30
NIST	1774092	0.004 214 789	-0.06	0.14
NPL	1728839	0.004419156	0.00	0.23
NRC	1872174	0.004 295 849	0.13	0.23
PTB	1842379	0.004 236 895	0.42	0.30
PTB*	1842381	0.004 238 681	0.08	0.30

Table 5.3: Comparison data near the 20.270 K calibration temperature.
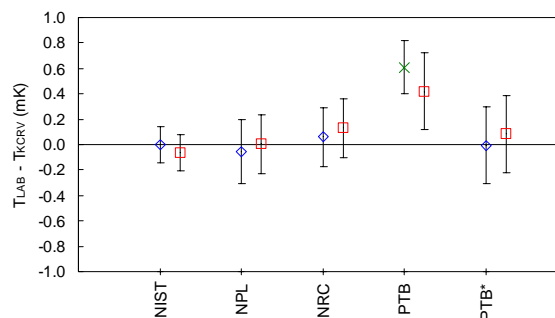
Figure 5.3: The comparison near the 20.270 K calibration temperature.

5.4   Near Ne TP

For the comparison near the neon triple point temperature, the cryostat was balanced within 0.2 mK of 24.5561 K for the Group A capsules, and within 2.7 mK for the Group B capsules.

KRISS reported a calibration value at this temperature, which is included in this analysis even though the absence of data at the hydrogen point means that their scale realization begins at 54 K.

As noted in the BNM-INM uncertainty budget, capsule 1041 was not very repeatable at the neon triple point: $u_L(1041,Ne) = 1.4$ mK. This is reflected in the graph of the comparison results shown below.

The scatter of the temperature differences, taken as a simple standard deviation of the *T-KCRV* values for both Group A and B thermometers (excluding the BNM-INM 1041 and PTB 1842381 data) is 0.13 mK.

Lab	S/N	W	T-$KCRV$	u_C
BNM	1886904	0.008 581 302	-0.02	0.54
IMGC	1857277	0.008 495 871	0.11	0.14
KRISS	1886906	0.008 523 028	0.01	0.20
NIST	1774095	0.008 633 474	-0.13	0.16
NPL	213865	0.008 507 130	-0.10	0.22
NRC	1872174	0.008 516 257	-0.06	0.22
PTB*	1842381	0.008 457 046	0.11	0.20
BNM	1041	0.008 524 861	-1.88	1.40
IMGC	1860951	0.008 500 855	0.11	0.14
KRISS	1043	0.008 511 365	-0.15	0.20
NIST	1774092	0.008 430 085	0.04	0.16
NPL	1728839	0.008 452 413	-0.19	0.19
NRC	1872174	0.008 513 109	-0.12	0.22
PTB	1842379	0.008 452 413	0.26	0.20
PTB*	1842381	0.008 454 102	0.21	0.20

Table 5.4: Comparison data near 24.5561 K, the neon triple point temperature.
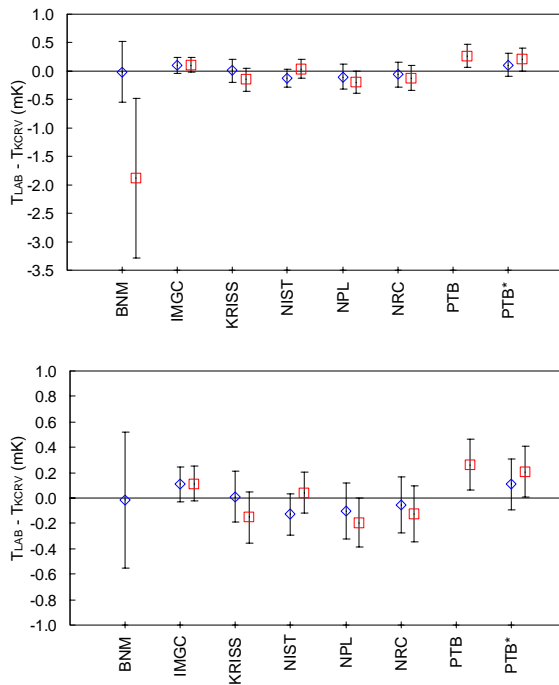
Figure 5.4: The comparison near 24.5561 K, the triple point of neon. An expanded-scale graph (excluding the Group B BNM point for thermometer 1041, which had the largest deviation from the baseline temperature) is also shown.

5.5   Near O_2 TP

For the comparison near the oxygen triple point temperature, the cryostat was balanced near 54.3584 K: within 0.5 mK for Group A, and within 0.7 mK for Group B.

The scatter of the temperature differences, taken as a simple standard deviation of the T-$KCRV$ values for both Group A and B thermometers (excluding the PTB 1842381 data) is 0.13 mK.

Lab	S/N	W	T-$KCRV$	u_C
BNM	1886904	0.091 851 621	-0.07	0.26
IMGC	1857277	0.091 842 149	-0.20	0.12
KRISS	1886906	0.091 817 050	0.09	0.17
NIST	1774095	0.091 915 678	0.07	0.10
NPL	213865	0.091 777 789	0.02	0.18
NRC	1872174	0.091 805 325	0.18	0.22
PTB*	1842381	0.091 742 965	-0.02	0.23
BNM	1041	0.091 816 645	0.01	0.25
IMGC	1860951	0.091 813 149	-0.16	0.12
KRISS	1043	0.091 805 357	0.10	0.17
NIST	1774092	0.091 730 552	-0.05	0.12
NPL	1728839	0.091 747 843	0.06	0.15
NRC	1872174	0.091 810 015	0.24	0.22
PTB	1842379	0.091 747 843	0.18	0.23
PTB*	1842381	0.091 748 090	0.15	0.23

Table 5.5: Comparison data near 54.3584 K, the oxygen triple point temperature.
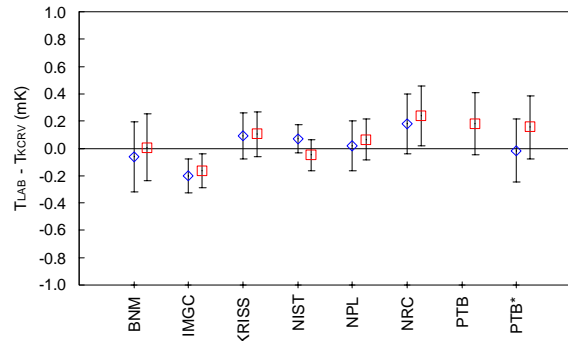
Figure 5.5: The comparison near 54.3584K, the triple point of oxygen.

5.6   Near Ar TP

Near the argon triple point temperature, the cryostat was balanced close to 83.8058 K for the comparison

measurements: within 0.7 mK for Group A, and within 0.2 mK for Group B.

The scatter of the temperature differences, taken as a simple standard deviation of the *T-KCRV* values for both Group A and B thermometers (excluding the PTB 1842381 data) is 0.19 mK.

Lab	S/N	W	*T-KCRV*	u_C
BNM	1886904	0.215 972 101	0.07	0.20
IMGC	1857277	0.215 981 409	-0.20	0.10
KRISS	1886906	0.215 949 212	0.55	0.17
NIST	1774095	0.216 038 028	0.00	0.10
NPL	213865	0.215 911 188	-0.03	0.17
NRC	1872174	0.215 941 946	0.18	0.22
PTB*	1842381	0.215 883 080	-0.15	0.19
BNM	1041	0.215 944 081	0.11	0.22
IMGC	1860951	0.215 944 525	-0.09	0.10
KRISS	1043	0.215 937 371	0.01	0.17
NIST	1774092	0.215 876 593	0.04	0.11
NPL	1728839	0.215 886 386	-0.04	0.13
NRC	1872174	0.215 944 613	0.24	0.22
PTB	1842379	0.215 886 386	0.22	0.21
PTB*	1842381	0.215 886 178	0.01	0.19

Table 5.6: Comparison data near 83.8058 K, the argon triple point temperature.
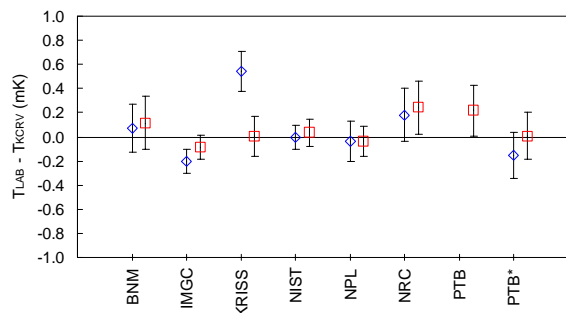
Figure 5.6: The comparison near 83.8058 K, the triple point of argon.

5.7   *Near Hg TP*

The mercury triple point temperature was the highest value at which both Groups of CSPRTs were compared in the cryostat. The block was balanced to within 0.2 mK of 234.3156 K for these comparison measurements.

The mercury point was problematic for some of the participants in this study: two of the laboratories experienced quite severe failures of their fixed point cells. In the case of BNM-INM, the corrective action

which was taken to update W(1041, Hg) value based on new measurements of W(1886904, Hg) in a good Hg cell have proved to be inadequate, and the deviations with respect to the *KCRV* for these two thermometers differ from each other by more than two standard uncertainties. For this reason, neither of the BNM-INM results is included in the calculation of the *KCRV*: they have been assigned zero weight. This does not impact on the utility or independence of these measurements in any way. Rather, excluding both was necessary to avoid creating an artificial difference in the comparison baseline between the Group A and Group B thermometers.

The scatter of the temperature differences, taken as a simple standard deviation of the *T-KCRV* values for both Group A and B thermometers (excluding the BNM 1041 and PTB 1842381 data) is 0.14 mK.

Lab	S/N	W	*T-KCRV*	u_C
BNM	1886904	0.844 163 638	-0.23	0.28
IMGC	1857277	0.844 167 763	-0.06	0.10
KRISS	1886906	0.844 159 979	-0.12	0.26
NIST	1774095	0.844 180 202	0.12	0.14
NPL	213865	0.844 152 407	0.11	0.19
NRC	1872174	0.844 160 883	-0.14	0.22
PTB*	1842381	0.844 146 571	0.05	0.17
BNM	1041	0.844 157 926	-0.87	0.28
IMGC	1860951	0.844 158 353	-0.07	0.10
KRISS	1043	0.844 157 290	0.23	0.26
NIST	1774092	0.844 146 607	0.09	0.12
NPL	1728839	0.844 146 812	-0.02	0.17
NRC	1872174	0.844 160 907	-0.14	0.22
PTB	1842379	0.844 146 812	0.06	0.19
PTB*	1842381	0.844 146 531	0.03	0.17

Table 5.7: The comparison near 234.3156 K, the triple point of mercury.
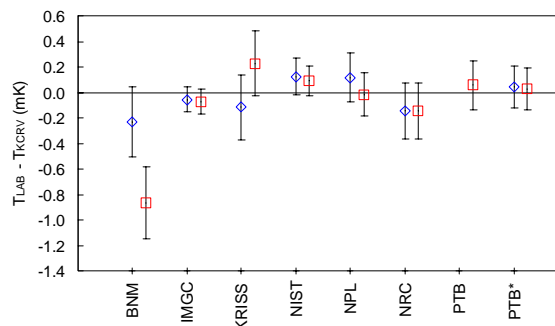
Figure 5.7: The comparison near 234.3156 K, the triple point of mercury.

5.8   Near H$_2$O TP

In order to test the utility of the cryostat for use at relatively high temperatures, a comparison run was made using the Group B thermometers only close to the triple point of water temperature. The cryostat was balanced approximately 6 mK above 273.16 K, and the usual round-robin measurements were performed. These data do not represent the independent national realizations of the TPW, since all are directly related to the resistance values obtained at the pilot laboratory. This is reflected in the comparison uncertainty column of Table 5.8, which is based on the NRC TPW uncertainty, rather than the individual laboratory uncertainties quoted in Section 2. The data presented here are not included in the Appendix B summary of the Key Comparison report for this reason. The data do, however, reinforce the high quality of the comparison data, and illustrate that the comparison cryostat may be operated successfully all the way up to 273 K. The scatter of the data, as given by the standard deviation, is only 64 μK; the standard deviation of the mean is 22 μK.

Lab	S/N	W	T-KCRV	u_C
BNM	1041	1.000 025 337	-0.03	0.18
IMGC	1860951	1.000 025 334	-0.03	0.18
KRISS	1043	1.000 025 649	0.05	0.18
NIST	1774092	1.000 025 486	0.01	0.18
NPL	1728839	1.000 025 653	0.00	0.18
NRC	1872174	1.000 025 665	0.05	0.18
PTB	1842379	1.000 025 653	0.05	0.18
PTB*	1842381	1.000 025 771	0.08	0.18

Table 5.8: The comparison near 273.16 K, the triple point of water.
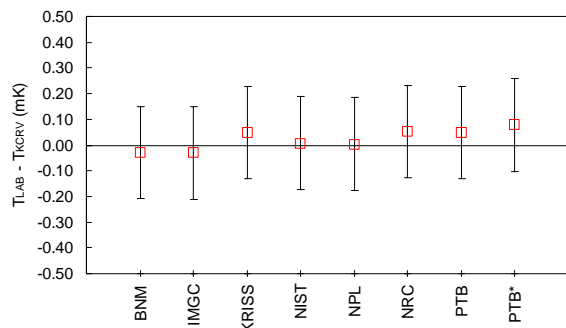
Figure 5.8: The comparison near 273.16 K, the triple point of water. Note that this experiment was done in the comparison block, and not in a TPW cell; also, the R(273.16K) values were measured at NRC.

5.9   Comparison Run Consistency

Two thermometers were included in both the Group A and the Group B comparison runs: NRC 1872174 and PTB 1842381. It is possible to exploit this fact to evaluate the experimental consistency between the two measurement runs. The temperature difference between these two thermometers should, ideally, be the same in the Group A and Group B data sets. The temperature difference between the two thermometers may be written as:

$$\delta = T(1872174) - T(1842381) \qquad (6)$$

and may be evaluated at each temperature using the Group A data (δ_A) and the Group B data (δ_B). In Figure 5.9, the differences between these two quantities, δ_A- δ_B, are plotted for each of the seven comparison temperatures. The error bars represent only the uncorrelated part of the comparison uncertainty, *i.e.* the experimental uncertainty components from Table 4.2. For temperatures below 20.3 K, the combined standard uncertainty for the differences, $u(\delta_A$- $\delta_B)$, is 0.24 mK; above this point, it is 0.18 mK. The calibration uncertainty for each of the thermometers cancels out due to the difference operation, making this technique a useful test of the experimental consistency and of the relative stability of these two thermometers. All of the data points are seen to coincide with the ideal to within their standard uncertainty.
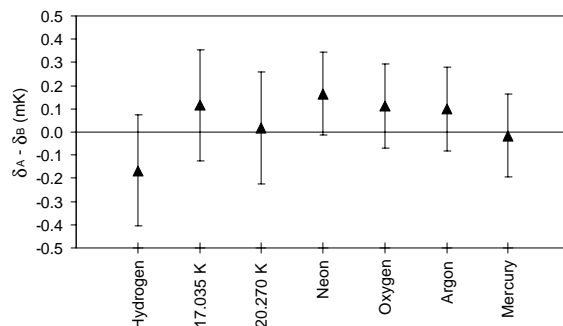
Figure 5.9: The consistency of the Group A and B comparison data, determined by examining the results for two thermometers included in both runs.

6.   SUMMARY OF FIXED-POINT DIFFERENCES BY NMI

In the following sections, the same data from Section 5 are presented on a single graph for each participating NMI. The tables and graphs are organized to provide a quick overview of the comparison differences and uncertainties for a single laboratory at each of the comparison points with

respect to the *KCRV* temperature values. The statistically-determined values for the *KCRV* temperatures in each Group were obtained using equivalent methods, and including corresponding capsules from the same laboratories. This means that the tables and graphs which follow can be used to evaluate not only the NMI-to-*KCRV* agreement, but the consistency of the two calibrations carried on the two thermometers for each NMI. The baseline value for each data set is numerically slightly different, but represents the same physical quantity, namely the weighted average temperature of the comparison block during each measurement.

6.1 BNM-INM

Two thermometers were provided by BNM-INM, and are summarized in the following table and graph.

	Group A		Group B	
	T-KCRV	$u_C(k=1)$	*T-KCRV*	$u_C(k=1)$
Hydrogen	-2.71	2.08	-2.60	2.08
17.035 K				
20.270 K				
Neon	-0.02	0.54	-1.88	1.40
Oxygen	-0.07	0.26	0.01	0.25
Argon	0.07	0.20	0.11	0.22
Mercury	-0.23	0.28	-0.87	0.28

Table 6.1: Two BNM-INM capsules compared to the *KCRV* at each fixed point.
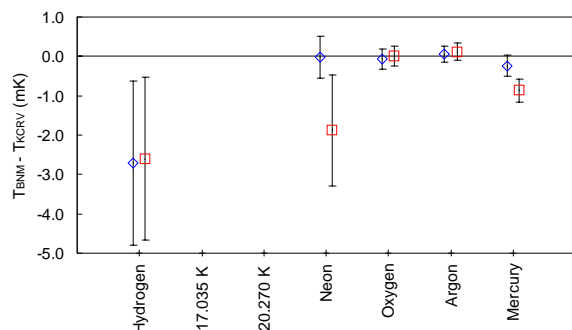
Figure 6.1: The observed differences between the capsules of BNM-INM and the *KCRV* at each of the defining fixed points. Data for BNM 1886904 is shown as the diamond (Group A), while BNM 1041 is the square (Group B).

6.2 IMGC

Two thermometers were provided by IMGC, and are summarized in the following table and graph.

	Group A		Group B	
	T-KCRV	$u_C(k=1)$	*T-KCRV*	$u_C(k=1)$
Hydrogen	-0.32	0.16	-0.17	0.16
17.035 K				
20.270 K				
Neon	0.11	0.14	0.11	0.14
Oxygen	-0.20	0.12	-0.16	0.12
Argon	-0.20	0.10	-0.09	0.10
Mercury	-0.06	0.10	-0.07	0.10

Table 6.2: Two IMGC capsules compared to the *KCRV* at each fixed point.
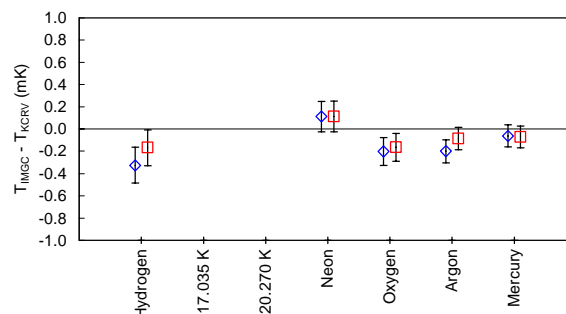
Figure 6.2: The observed differences between the capsules of IMGC and the *KCRV* at each of the defining fixed points. Data for IMGC 1857277 is shown as the diamond (Group A), while IMGC 1860951 is the square (Group B).

6.3 KRISS

Two thermometers were provided by KRISS, and are summarized in the following table and graph.

	Group A		Group B	
	T-KCRV	$u_C(k=1)$	*T-KCRV*	$u_C(k=1)$
Hydrogen				
17.035 K				
20.270 K				
Neon	0.01	0.20	-0.15	0.20
Oxygen	0.09	0.17	0.10	0.17
Argon	0.55	0.17	0.01	0.17
Mercury	-0.12	0.26	0.23	0.26

Table 6.3: Two KRISS capsules compared to the *KCRV* at each fixed point.
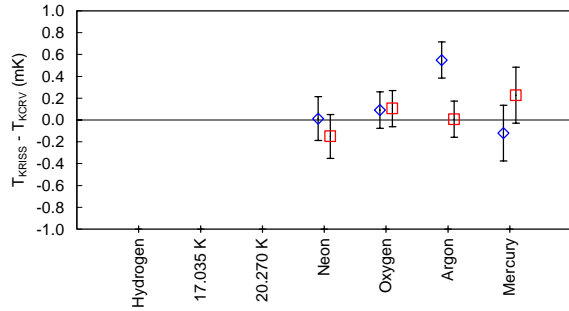
Figure 6.3: The observed differences between the capsules of KRISS and the *KCRV* at each of the defining fixed points. Data for KRISS 1886906 is shown as the diamond (Group A), while KRISS 1043 is the square (Group B).

6.4   NIST

Two thermometers were provided by NIST, and are summarized in the following table and graph.

	Group A		Group B	
	T-KCRV	$u_C(k=1)$	*T-KCRV*	$u_C(k=1)$
Hydrogen	0.42	0.17	0.42	0.17
17.035 K	-0.01	0.15	0.01	0.15
20.270 K	0.00	0.14	-0.06	0.14
Neon	-0.13	0.16	0.04	0.16
Oxygen	0.07	0.10	-0.05	0.12
Argon	0.00	0.10	0.04	0.11
Mercury	0.12	0.14	0.09	0.12

Table 6.4: Two NIST capsules compared to the *KCRV* at each fixed point.
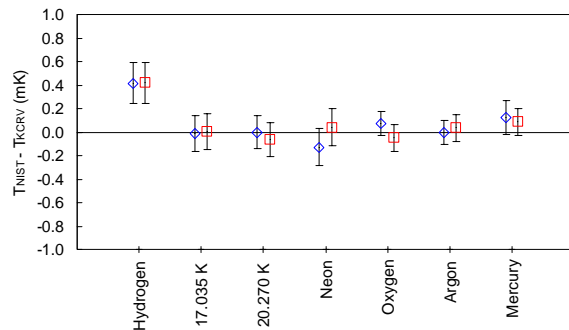
Figure 6.4: The observed differences between the capsules of NIST and the *KCRV* at each of the defining fixed points. Data for NIST 1774095 is shown as the diamond (Group A), while 1774092 is the square (Group B).

6.5   NPL

Two thermometers were provided by NPL, and are summarized in the following table and graph.

	Group A		Group B	
	T-KCRV	$u_C(k=1)$	*T-KCRV*	$u_C(k=1)$
Hydrogen	0.07	0.21	-0.05	0.18
17.035 K	0.06	0.25	-0.09	0.23
20.270 K	-0.06	0.25	0.00	0.23
Neon	-0.10	0.22	-0.19	0.19
Oxygen	0.02	0.18	0.06	0.15
Argon	-0.03	0.17	-0.04	0.13
Mercury	0.11	0.19	-0.02	0.17

Table 6.5: Two NPL capsules compared to the *KCRV* at each fixed point.
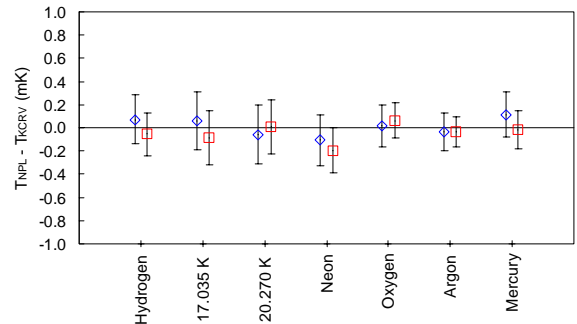
Figure 6.5: The observed differences between the capsules of NPL and the *KCRV* at each of the defining fixed points. Data for NPL 213865 is shown as the diamond (Group A), while NPL 1728839 is the square (Group B).

6.6   NRC

The same NRC capsule was included in both experimental Groups, and therefore these data provide information regarding the consistency of the two *KCRV* values for each Group. It is clear from Figure 6.6 that the run to run consistency is quite good, and well within the experimental comparison uncertainty.

	Group A		Group B	
	T-KCRV	$u_C(k=1)$	*T-KCRV*	$u_C(k=1)$
Hydrogen	-0.26	0.23	-0.27	0.23
17.035 K	0.05	0.23	0.18	0.23
20.270 K	0.06	0.23	0.13	0.23
Neon	-0.06	0.22	-0.12	0.22
Oxygen	0.18	0.22	0.24	0.22
Argon	0.18	0.22	0.24	0.22
Mercury	-0.14	0.22	-0.14	0.22

Table 6.6: One NRC capsule compared to the *KCRV* at each fixed point.
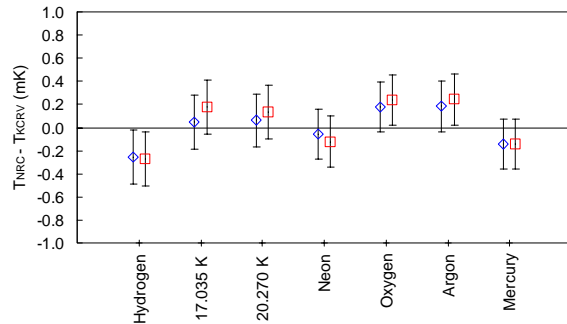
Figure 6.6: The observed differences between the capsule of NRC and the *KCRV* at each of the defining fixed points. The thermometer NRC 1872174 was used in both Groups A and B, and therefore this graph shows the run-to-run consistency of the data acquisition system.

6.7 PTB

The two PTB capsules are represented in the following table and figure. It is important to remember that capsule PTB 1842381 has been subject to a correction, δR, for a shift in the temperature-independent residual resistance. This means that the scale as carried by this capsule is no longer a straightforward representation of the ITS-90 as realized by PTB. Nevertheless, data on this capsule provide information about the stability of the calibration on PTB 1842379, since the two capsules are seen to agree to within experimental error at all of the comparison points. Only the data for PTB 1842379 are included in the Appendix B summary.

	Group A		Group B	
	T-KCRV	$u_C(k=1)$	*T-KCRV*	$u_C(k=1)$
Hydrogen	0.16	0.26	-0.02	0.26
17.035 K	-0.04	0.31	0.13	0.31
20.270 K	0.00	0.30	0.08	0.30
Neon	0.11	0.20	0.21	0.20
Oxygen	-0.02	0.23	0.15	0.23
Argon	-0.15	0.19	0.01	0.19
Mercury	0.05	0.17	0.03	0.17

	Group B	
	T-KCRV	$u_C(k=1)$
Hydrogen	-0.02	0.22
17.035 K	0.21	0.30
20.270 K	0.42	0.30
Neon	0.26	0.20
Oxygen	0.18	0.23
Argon	0.22	0.21
Mercury	0.06	0.19

Table 6.7: Two PTB capsules compared to the *KCRV* at each fixed point. Top: PTB 1842381 has been corrected for a change in the residual resistance during this work. Bottom: PTB 1842379 as included in the Appendix B summary.
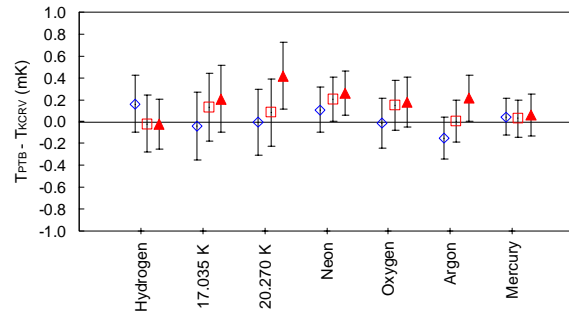
Figure 6.7: The observed differences between the capsule of PTB and the *KCRV* at each of the defining fixed points. The values for PTB 1842379 in Group B are shown as solid triangles. The corrected thermometer PTB 1842381 values are shown as a consistency check, with symbols Group A: open diamond, Group B: open square.

7. SCALE NON-UNIQUENESS INVESTIGATION

The deviation function coefficients were calculated at NRC. In order to eliminate any artificial scale differences caused by the purely-numerical subrange inconsistency problem, full 13.8033 K to 273.16 K range deviation equations were determined for all of

the capsules, including those supplied with a limited-range calibration. To achieve this, the *W* values as determined in the comparison block were used to supply the missing calibration points.

The Group A thermometers were measured at over eighty temperature comparison points in a period of several weeks. The spirit and intent of this portion of the comparison is that of Ward and Compton [6] and the recent Euromet comparison of Head.[7] Figure 7.1 is directly comparable to Figure 4.1 from Section 4.3, since it covers the same temperature range, and includes thermometers from the same group of four laboratories (NIST, NPL, NRC, and PTB). In Figure 7.2, the comparison results over the entire temperature range are shown on a semi-logarithmic plot, with the fixed point temperatures indicated by the triangles to give the scale. The overall smoothness of the data, and the general agreement of the various national realizations of the ITS-90 is quite good. These data will be analyzed more completely in a subsequent publication.
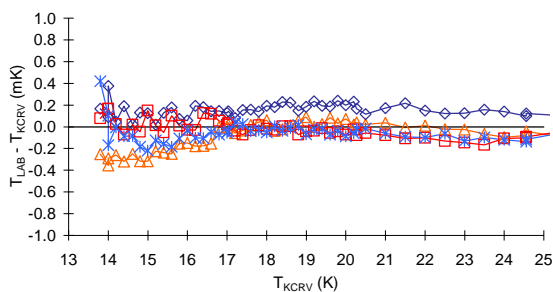
Figure 7.1: Temperature deviations for four capsule thermometers at the low end of the platinum range in ITS-90. The symbol key for this graph is: triangle = NRC 1872174; diamond = PTB 1842381; square = NPL 213865; star = NIST 1774095.
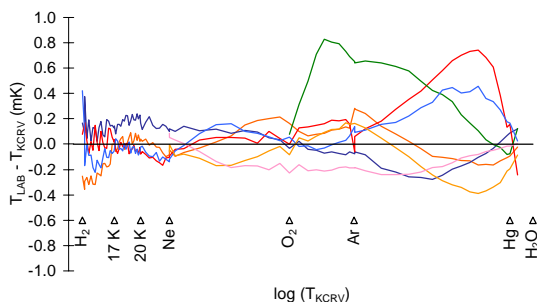
Figure 7.2: Temperature deviations for seven capsule thermometers at several intermediate temperatures between each of the calibration points (indicated by triangles).

8. CONCLUSIONS

Calibrated capsule-style standard platinum resistance thermometers have been used to compare the realizations of the low-temperature portion of the International Temperature Scale of 1990 for seven countries. Comparison measurements have been made at temperatures near the ITS-90 defining fixed point temperatures for two separate groups of thermometers. The degree of equivalence of the national scale realizations as carried on the thermometers has been measured and summarized in a convenient tabular form, suitable for creating a database entry for Appendix B to the CIPM Mutual Recognition Arrangement. The measurements made here are complementary to the on-going comparison of sealed-cell fixed points, which form the basis for the national calibration services.

Virtually every thermometer in this Key Comparison agrees with the *KCRV* temperature at every ITS-90 fixed point temperature to within the expanded (*k*=2) comparison uncertainty, and all but a few agree to within the comparison uncertainty. Some of this latter group (such as the BNM-INM deviations at the hydrogen point, for example) have essentially no impact on the quality of the scale being disseminated via calibrations performed in that laboratory due to the reduction in the propagated uncertainty at higher temperatures. The comparison results at the fixed points show variability among the different realizations which have been calculated as simple standard deviations of the *T-KCRV* values of 0.28 mK at hydrogen, 0.16 mK at 17 K, 0.23 mK at 20.3 K, 0.13 mK at neon, 0.13 mK at oxygen, 0.19 mK at argon, and 0.14 mK at mercury. These values may be thought of as characterizing the differences among the realizations of the various fixed points used by the participants of this comparison, in the same way that the "cell-comparison dispersion" values obtained in the 1984 international comparison of fixed points by means of sealed cells [9] summarized what was then the state-of-the-art in low temperature thermometry. The data presented here are comparable to the best results of that study, and indicate that, with care, successful comparisons can be carried out using thermometers as the transfer mechanism.

This comparison has been quite a major undertaking, lasting well over four years and involving many hundreds of precision measurements. The results are very successful, and illustrate the very high level of equivalence of the various national realizations of the International Temperature Scale of 1990.

9. ACKNOWLEDGEMENTS

10. REFERENCES

[1] H. Preston-Thomas, *Metrologia*, 1990, **27**, 3-10 and 107 (erratum).

[2] "Mutual recognition of national measurement standards and of calibration and measurement certificates issued by national metrology institutes", Comité International des Poids et Mesures, Paris, (14 October 1999).

[3] A.G. Steele, Proceedings of *Low Temperature Thermometry and Dynamic Temperature Measurement* (Wroclaw, Poland), L48–L53 (1997).

[4] C.W. Meyer, G.F. Strouse, and W.L. Tew, Proceedings of *Tempmeko '99*, 91-94 (1999).

[5] D.I. Head, NPL, *private communication*

[6] S.D. Ward and J.P. Compton, *Metrologia*, 1979, **15**, 31-46.

[7] D.I. Head, Proceedings of *Low Temperature Thermometry and Dynamic Temperature Measurement* (Wroclaw, Poland), L36–L41 (1997).

[8] B.M. Wood and R.J. Douglas, *Metrologia*, 1998, **35**, 187-196 ; Erratum : *Metrologia*, 1999, **36**, 245.

[9] F. Pavese, J. Ancsin, D.N. Astrov, J. Bonhoure, G. Bonnier, G.T. Furukawa, R.C. Kemp, H. Maas, R.L. Rusby, H. Sakurai, and Ling Shan-Kang, *Metrologia*, 1984, **20**, 127-144.

APPENDIX A
The detailed uncertainty budgets for the participating NMIs are listed here.

Capsule: 1886904

Fixed-point	H_2	17 K	20.3 K	Ne	O_2	Ar	Hg	H_2O
Substance purity	6N			4N	5N5	6N	7N	
Uncertainty components, Type B estimate (mK)								
Repeatability	0.20	-	-	0.06	0.06	0.04	0.08	0.10
Electrical measurement	0.10	-	-	0.10	0.05	0.05	0.05	0.05
Self heating	0.05	-	-	0.05	0.05	0.05	0.05	0.05
Spurious heat flux	0.50	-	-	0.10	0.05	0.05	0.10	0.10
Hydrostatic pressure effect	0.00	-	-	0.00	0.00	0.00	0.07	0.01
Interpretation of the plateau	0.20	-	-	0.10	0.07	0.05	0.05	0.05
Triple point value	2.00	-	-	0.50	0.20	0.15	0.20	0.10
Type B combined uncertainty (mK)	2.08	-	-	0.53	0.24	0.18	0.26	0.19
Uncertainty components, Type A estimate (mK)								
Type A combined uncertainty (mK)	-	-	-	-	-	-	-	-
Standard combined uncertainty (mK)	2.08	-	-	0.53	0.24	0.18	0.26	0.19
Expanded uncertainty ($k=2$) (mK)	4.17	-	-	1.07	0.47	0.37	0.52	0.38

Capsule: 1041

Fixed-point	H_2	17 K	20.3 K	Ne	O_2	Ar	Hg	H_2O
Substance purity	6N			4N	5N5	6N	7N	
Uncertainty components, Type B estimate (mK)								
Repeatability	0.10	-	-	1.30	0.03	0.09	0.10	0.02
Electrical measurement	0.10	-	-	0.10	0.05	0.05	0.05	0.05
Self heating	0.05	-	-	0.05	0.05	0.05	0.05	0.05
Spurious heat flux	0.50	-	-	0.10	0.05	0.05	0.10	0.10
Hydrostatic pressure effect	0.00	-	-	0.00	0.00	0.00	0.07	0.01
Interpretation of the plateau	0.20	-	-	0.10	0.07	0.05	0.05	0.05
Triple point value	2.00	-	-	0.50	0.20	0.15	0.20	0.10
Correction by comparison	-	-	-	-	-	-	0.05	-
Type B combined uncertainty (mK)	2.08	-	-	1.40	0.23	0.20	0.27	0.17
Uncertainty components, Type A estimate (mK)								
Type A combined uncertainty (mK)	-	-	-	-	-	-	-	-
Standard combined uncertainty (mK)	2.08	-	-	1.40	0.23	0.20	0.27	0.17
Expanded uncertainty ($k=2$) (mK)	4.15	-	-	2.81	0.46	0.40	0.54	0.33

Table A.1: Uncertainty budget for BNM-INM thermometers.

Capsules: 1857277 and 1860951

Fixed-point		H$_2$	17 K	20.3K	Ne	O$_2$	Ar	Hg	H$_2$O
Substance purity		6N			4N5	4N8	5N7	7N	7N
Uncertainty components, Type B estimate (mK)									
Ref Std. Resistor (10 Ω)	(-)	-			-	-	-	-	-0.019
	(+)	-			-	-	-	-	+0.019
Comparison Resistor (1 to 10 Ω)	(-)	-0.030			-0.010	-	-	-0.000	-0.015
	(+)	+0.030			+0.010	-	-	+0.000	+0.015
Bridge Ratio (therm.)	(-)	-0.000			-0.000	-0.003	-0.003	-0.007	-0.007
	(+)	+0.000			+0.000	+0.003	+0.003	+0.007	+0.007
Std. Resistor temp stability	(-)	-0.030			-0.000	-0.001	-0.001	-0.010	-0.006
	(+)	+0.030			+0.000	+0.001	+0.001	+0.010	+0.006
Self-heating error	(-)	-0.010			-0.010	-0.010	-0.010	-0.010	-0.010
	(+)	+0.010			+0.010	+0.010	+0.010	+0.010	+0.010
Quadrature Effects	(-)	-0.040			-0.010	-0.002	-0.002	-0.004	-0.004
	(+)	+0.000			+0.000	+0.000	+0.000	+0.000	+0.004
Hydrogen Conversion	(-)	-0.010			-	-	-	-	-
	(+)	+0.000			-	-	-	-	-
Isotopic Composition	(-)	-			-0.050	-	-	-	-
	(+)	-			+0.050	-	-	-	-
Thermal Leak	(-)	-0.015			-0.015	-0.010	-0.010	-0.005	-0.005
	(+)	+0.000			+0.000	+0.000	+0.000	+0.000	+0.000
Impurities	(-)	-0.000			-0.000	-0.000	-0.000	-0.000	-0.000
	(+)	+0.005			+0.050	+0.000	+0.030	+0.010	+0.005
Cell-to-cell Correction	(-)	-			-	-0.075	-	-	-
	(+)	-			-	+0.075	-	-	-
Recrystallization Effect	(-)	-			-	-	-	-	-0.002
	(+)	-			-	-	-	-	+0.000
Hydrostatic Head Correction	(-)	-0.005			-0.020	-0.015	-0.033	-0.018	-0.002
	(+)	+0.000			+0.000	+0.000	+0.000	+0.018	+0.002
Triple Point Evaluation	(-)	-			-	-	-	-	-0.005
	(+)	-			-	-	-	-	+0.005
TPW Propagation	(-)	-0.001			-0.001	-0.003	-0.007	-0.030	-
	(+)	+0.001			+0.001	+0.003	+0.007	+0.030	-
Type B combined uncertainty (mK)	(-)	-0.062			-0.059	-0.078	-0.037	-0.039	-0.029
	(+)	+0.044			+0.072	+0.076	+0.033	+0.040	+0.029
Uncertainty components, Type A estimate (mK)									
(Bridge Reading: not used)	(-)	-0.070			-0.030	-0.021	-0.017	-0.003	-0.003
	(+)	+0.070			+0.030	+0.021	+0.017	+0.003	+0.003
Plateau reproducibility	(-)	-0.095			-0.085	-0.029	-0.042	-0.031	-0.020
	(+)	+0.095			+0.085	+0.029	+0.042	+0.031	+0.020
Type A combined uncertainty (mK)	(-)	-0.095			-0.085	-0.029	-0.042	-0.031	-0.020
	(+)	+0.095			+0.085	+0.029	+0.042	+0.031	+0.020
Standard combined uncertainty (mK)	(-)	-0.113			-0.103	-0.083	-0.056	-0.050	-0.035
	(+)	+0.105			+0.111	+0.081	+0.053	+0.050	+0.035
Expanded uncertainty ($k=2$) (mK)	(-)	-0.227			-0.206	-0.166	-0.112	-0.099	-0.071
	(+)	+0.209			+0.223	+0.162	+0.106	+0.101	+0.070

Table A.2: Uncertainty budget for IMGC thermometers.

Capsules: 1886906 and 1043

Fixed-point	H_2	17 K	20.3 K	Ne	O_2	Ar	Hg	H_2O
Substance purity	-	-	-	4N4	4N8	5N5	7N8	-
Uncertainty components, Type B estimate (mK)								
Chemical impurities	-	-	-					
and Isotopic Differences	-	-	-	0.15	0.10	0.05	0.03	0.03
Determination of TP value	-	-	-					
hydrostatic effect, and	-	-	-					
self-heating correction	-	-	-	0.05	0.05	0.05	0.05	0.05
Accuracy of bridge, and								
standard resistor accuracy	-	-	-	0.05	0.05	0.05	0.05	0.05
Type B combined uncertainty (mK)	-	-	-	0.17	0.12	0.09	0.08	0.08
Uncertainty components, Type A estimate (mK)								
Bridge reading	-	-	-	0.05	0.05	0.05	0.05	0.05
Plateau reproducibility	-	-	-	0.05	0.05	0.10	0.10	0.05
Scatter of measurements							0.20	
Type A combined uncertainty (mK)	-	-	-	0.07	0.07	0.11	0.23	0.07
Standard combined uncertainty (mK)	-	-	-	0.18	0.14	0.14	0.24	0.10
Expanded Uncertainty (*k=2*)	-	-	-	0.36	0.28	0.28	0.48	0.21

Table A.3: Uncertainty budget for KRISS thermometers.

Capsule: 1774095

Fixed-point	H$_2$	17 K	20.3 K	Ne	O$_2$	Ar	Hg	H$_2$O
Uncertainty components, Type A estimate (mK)								
repeatability of FP realizations	0.064	0.050	0.050	0.091	0.04	0.040	0.1	0.025
repeatability of comparisons	0.048	0.035	0.031	0.025				
repeatability of ref. therm.	0.048	0.035	0.031	0.025				
Type A combined uncertainty (mK)	0.093	0.071	0.067	0.097	0.040	0.040	0.100	0.025
Uncertainty components, Type B estimate (mK)								
Realizations								
Chemical Impurities u				0.014	0.003	0.017	0.010	0.003
Chemical Impurities b				0.025		0.030		
Isotopic Variations	*	*	*	0.075				0.003
static-head correction							0.041	0.005
Immersion	0.020			0.020	0.020	0.006	0.007	0.003
Thermal Equilibrium	0.020	0.010	0.010	0.020	0.010	0.010	0.020	
Spin/Phase Equilibrium u	0.012	0.012	0.012					
Spin/Phase Equilibrium b	-0.020	-0.020	-0.020					
Pressure Gauge Cal.		0.042	0.032					
Comparison								
Thermal Gradients	0.001	0.002	0.003	0.004				
Reference Therm. Meas.	0.051	0.026	0.013	0.018				
Temperature Corrections	0.020			0.020				
Stability / Drift	0.010	0.010	0.010	0.020				
Measurement								
bridge accuracy	0.001	0.001	0.001	0.001	0.004	0.009	0.005	0.030
frequency dependence u	0.051	0.025	0.010	0.017				
frequency dependence b	-0.086	-0.055	-0.029	-0.020				
resistance standards	0.0019	0.002	0.002	0.0024	0.016			0.064
SPRT self-heating	0.003	0.006	0.008	0.004	0.003	0.003	0.007	0.035
Propagated H$_2$O TP	0.001	0.001	0.001	0.001	0.002	0.005	0.022	
Type B combined uncertainty (mK)	0.082	0.058	0.041	0.090	0.028	0.024	0.053	0.079
b$_{net}$	-0.106	-0.075	-0.049	0.005	0.000	0.030	0.000	0.000
Standard combined uncertainty (mK)	0.124	0.092	0.078	0.132	0.049	0.046	0.113	0.083
Expanded uncertainty (k=2) (mK)	0.248	0.183	0.157	0.265	0.098	0.093	0.227	0.166
Total Asymmetric Expanded + (k=2)	0.142	0.108	0.107	0.269	0.098	0.123	0.227	0.166
Total Asymmetric Expanded - (k=2)	-0.354	-0.258	-0.206	-0.260	-0.098	-0.063	-0.227	-0.166

Table A.4.1: Uncertainty budget for NIST thermometers. Some asymmetric uncertainty components (labelled "b")
are identified as introducing a bias; the corresponding symmetric value has been calculated assuming no bias
(labelled "u"). The asymmetric expanded uncertainty is reported for information only ; the (symmetric) standard
combined uncertainty is used throughout this report.

Capsule: 1774092

Fixed-point	H_2	17 K	20.3 K	Ne	O_2	Ar	Hg	H_2O
Uncertainty components, Type A estimate (mK)								
repeatability of FP realizations	0.064	0.050	0.050	0.091	0.014	0.050	0.05	0.025
repeatability of comparisons	0.048	0.035	0.031	0.025	0.025			
repeatability of ref. therm.	0.048	0.035	0.031	0.025	0.025			
Type A combined uncertainty (mK)	0.093	0.071	0.067	0.097	0.038	0.050	0.050	0.025
Uncertainty components, Type B estimate (mK)								
Realizations								
Chemical Impurities u				0.014	0.003	0.020	0.010	0.003
Chemical Impurities b				0.025		0.030		
Isotopic Variations	*	*	*	0.075				0.003
static-head correction						0.018	0.041	0.005
Immersion	0.020			0.020	0.010	0.030	0.007	0.003
Thermal Equilibrium	0.020	0.010	0.010	0.020	0.020	0.020	0.020	
Spin/Phase Equilibrium u	0.012	0.012	0.012					
Spin/Phase Equilibrium b	-0.020	-0.020	-0.020					
Pressure Gauge Cal.		0.042	0.032					
Comparison								
Thermal Gradients	0.001	0.002	0.003	0.004	0.027			
Reference Therm. Meas.	0.051	0.026	0.013	0.018	0.023			
Temperature Corrections	0.020			0.020	0.020			
Stability / Drift	0.010	0.010	0.010	0.020	0.035			
Measurement								
bridge accuracy	0.001	0.001	0.001	0.001	0.004	0.009	0.005	0.030
frequency dependence u	0.051	0.025	0.010	0.017				
frequency dependence b	-0.086	-0.055	-0.029	-0.020				
resistance standards	0.0019	0.002	0.002	0.0024	0.016			0.064
SPRT self-heating	0.003	0.006	0.008	0.004	0.003	0.003	0.007	0.035
Propagated H_2O TP	0.001	0.001	0.001	0.001	0.002	0.005	0.022	
Type B combined uncertainty (mK)	0.082	0.058	0.041	0.090	0.061	0.046	0.053	0.079
b_{net}	-0.106	-0.075	-0.049	0.005	0.000	0.030	0.000	0.000
Standard combined uncertainty (mK)	0.124	0.092	0.078	0.132	0.072	0.068	0.073	0.083
Expanded uncertainty (k=2) (mK)	0.248	0.183	0.157	0.265	0.143	0.136	0.146	0.166
Total Asymmetric Expanded + (k=2)	0.142	0.108	0.107	0.269	0.143	0.166	0.146	0.166
Total Asymmetric Expanded - (k=2)	-0.354	-0.258	-0.206	-0.260	-0.143	-0.106	-0.146	-0.166

Table A.4.2: Uncertainty budget for NIST thermometers. Some asymmetric uncertainty components (labelled "b")
are identified as introducing a bias; the corresponding symmetric value has been calculated assuming no bias
(labelled "u"). The asymmetric expanded uncertainty is reported for information only ; the (symmetric) standard
combined uncertainty is used throughout this report.

Capsule: 213865

Fixed-point	H_2	17 K	20.3 K	Ne	O_2	Ar	Hg	H_2O
Substance purity	6N	-	-	5N	4N8	6N	6N	-
Uncertainty components, Type B estimate (mK)								
Chemical impurities	0.02	-	-	0.02	0.10	0.05	0.04	0.03
Isotopic differences	-	-	-	0.15	-	-	-	0.02
Molecular equilibration	0.05	-	-	-	-	-	-	-
Determination of TP value	0.03	-	-	0.03	0.03	0.03	0.03	0.03
Hydrostatic effect	<0.01	-	-	<0.02	<0.02	<0.03	0.02	0.010
Effect of heat-fluxes	0.02			0.02	0.03	0.03	0.03	0.04
Self-heating correction	0.02	-	-	0.02	0.02	0.02	0.03	0.03
Accuracy of bridge ratio	0.05	-	-	0.02	0.01	0.01	0.05	0.05
Standard resistor accuracy	<0.01	-	-	<0.01	0.01	0.02	0.02	0.02
Standard resistor temperature	<0.01	-	-	<0.01	<0.01	<0.01	0.01	0.01
Uncertainty propagation from TPW	<0.01	-	-	<0.01	0.01	0.02	0.09	-
Calibration by Comparison	0.10	0.10	0.10	0.10	0.10	0.10	0.10	
Type B combined uncertainty (mK)	0.13	0.22	0.22	0.19	0.15	0.12	0.16	0.09
Uncertainty components, Type A estimate (mK)								
Bridge reading	0.10	-	-	0.03	0.02	0.02	0.03	0.03
Plateau reproducibility	0.05	-	-	0.05	0.05	0.05	0.05	0.05
Type A combined uncertainty (mK)	0.11	-	-	0.06	0.05	0.05	0.06	0.06
Standard combined uncertainty (mK)	0.17	0.22	0.22	0.20	0.16	0.14	0.17	0.11
Expanded Uncertainty ($k=2$)	0.34	0.45	0.45	0.39	0.32	0.27	0.34	0.21

Capsule: 1728839

Fixed-point	H_2	17 K	20.3 K	Ne	O_2	Ar	Hg	H_2O
Substance purity	6N	-	-	5N	4N8	6N	6N	-
Uncertainty components, Type B estimate (mK)								
Chemical impurities	0.02	-	-	0.02	0.10	0.05	0.04	0.03
Isotopic differences	-	-	-	0.15	-	-	-	0.02
Molecular equilibration	0.05	-	-	-	-	-	-	-
Determination of TP value	0.03	-	-	0.03	0.03	0.03	0.03	0.03
Hydrostatic effect	<0.01	-	-	<0.02	<0.02	<0.03	0.02	0.010
Effect of heat-fluxes	0.02			0.02	0.03	0.03	0.03	0.04
Self-heating correction	0.02	-	-	0.02	0.02	0.02	0.03	0.03
Accuracy of bridge ratio	0.05	-	-	0.02	0.01	0.01	0.05	0.05
Standard resistor accuracy	<0.01	-	-	<0.01	0.01	0.02	0.02	0.02
Standard resistor temperature	<0.01	-	-	<0.01	<0.01	<0.01	0.01	0.01
Uncertainty propagation from TPW	<0.01	-	-	<0.01	0.01	0.02	0.09	-
Type B combined uncertainty (mK)	0.08	0.20	0.20	0.16	0.11	0.07	0.13	0.09
Uncertainty components, Type A estimate (mK)								
Bridge reading	0.10	-	-	0.03	0.02	0.02	0.03	0.03
Plateau reproducibility	0.05	-	-	0.05	0.05	0.05	0.05	0.05
Type A combined uncertainty (mK)	0.11	-	-	0.06	0.05	0.05	0.06	0.06
Standard combined uncertainty (mK)	0.14	0.20	0.20	0.17	0.12	0.09	0.14	0.11
Expanded Uncertainty ($k=2$)	0.28	0.40	0.40	0.34	0.25	0.18	0.28	0.21

Table A.5: Uncertainty budget for NPL thermometers.

Capsule: 1872174

Fixed-point	H_2	17 K	20.3 K	Ne	O_2	Ar	Hg	H_2O
Nominal substance purity	5N	-	-	5N	5N	5N5	6N5	-
Uncertainty components, Type B estimate (mK)								
Chemical impurities, isotopes	0.16	-	-	0.16	0.16	0.15	0.07	0.05
Determination of TP value	0.07	-	-	0.05	0.05	0.05	0.03	0.05
Hydrostatic effect; gas pressure	0.01	-	-	0.03	0.03	0.05	0.05	0.02
Effect of heat-fluxes	0.02			0.02	0.02	0.02	0.15	0.07
Self-heating correction	0.02	-	-	0.02	0.02	0.02	0.02	0.05
Accuracy of bridge ratio	0.04	-	-	0.04	0.04	0.04	0.04	0.04
Standard resistor	0.01	-	-	0.01	0.01	0.01	0.01	0.05
Uncertainty propagation from TPW	0.002	-	-	0.002	0.003	0.01	0.03	-
Type B combined uncertainty (mK)	0.18	0.19	0.19	0.18	0.18	0.17	0.18	0.13
Type A combined uncertainty (mK)	0.07	0.07	0.07	0.07	0.07	0.07	0.07	0.07
Standard combined uncertainty (mK)	0.2	0.2	0.2	0.2	0.2	0.2	0.2	0.15
Expanded Uncertainty ($k=2$)	0.4	0.4	0.4	0.4	0.4	0.4	0.4	0.3

Table A.6: Uncertainty budget for NRC thermometer.

Capsule: 1842379

Fixed-point	H_2	17 K	20.3 K	Ne	O_2	Ar	Hg	H_2O
Highest purity	6N	DCGT	DCGT	5N	6N	6N	6N	
Immersion depth / cm	2.5			2.5	2.5	2.5	2.5	19
Uncertainty components, Type B estimate (mK)								
Chemical impurities, isotopes	0.17			0.16	0.19	0.14	0.06	0.04
Reference scale (DCGT)		0.27	0.27					
Hydrostatic head correction	0.005			0.02	0.02	0.04	0.03	0.004
Error in gas pressure							0.01	0.005
Standard resistor	0.001	0.001	0.001	0.001	0.002	0.003	0.01	0.04
Bridge measurement	0.04	0.03	0.02	0.01	0.01	0.01	0.05	0.015
Uncertainty propagation from TPW	0.002	0.002	0.002	0.003	0.01	0.02	0.07	
Self-heating error	0.02	0.02	0.02	0.02	0.02	0.02	0.05	0.04
Heat-flux immersion error	0.02			0.02	0.02	0.02	0.02	0.01
Temperature inhomogeneity		0.05	0.05					
Choice of fixed-point value	0.05			0.05	0.05	0.05	0.05	0.01
Drift correction		0.03	0.03					
Stability at TPW (added by CCT-K2)						0.10	0.10	
Type B combined uncertainty (mK)	0.18	0.28	0.28	0.17	0.20	0.19	0.17	0.07
Type A combined uncertainty (mK)	0.05	0.05	0.05	0.05	0.05	0.05	0.05	0.03
Standard combined uncertainty (mK)	0.19	0.28	0.28	0.18	0.21	0.19	0.17	0.08
Expanded uncertainty ($k=2$) (mK)	0.38	0.56	0.56	0.36	0.41	0.39	0.35	0.16

Capsule: 1842381

Fixed-point	H_2	17 K	20.3 K	Ne	O_2	Ar	Hg	H_2O
Highest purity	6N	DCGT	DCGT	5N	6N	6N	6N	
Immersion depth / cm	2.5			2.5	2.5	2.5	2.5	19
Uncertainty components, Type B estimate (mK)								
Chemical impurities, isotopes	0.17			0.16	0.19	0.14	0.06	0.04
Reference scale (DCGT)		0.27	0.27					
Hydrostatic head correction	0.005			0.02	0.02	0.04	0.03	0.004
Error in gas pressure							0.01	0.005
Standard resistor	0.001	0.001	0.001	0.001	0.002	0.003	0.01	0.04
Bridge measurement	0.04	0.03	0.02	0.01	0.01	0.01	0.05	0.015
Uncertainty propagation from TPW	0.002	0.002	0.002	0.003	0.01	0.02	0.07	
Self-heating error	0.02	0.02	0.02	0.02	0.02	0.02	0.05	0.04
Heat-flux immersion error	0.02			0.02	0.02	0.02	0.02	0.01
Temperature inhomogeneity		0.05	0.05					
Choice of fixed-point value	0.05			0.05	0.05	0.05	0.05	0.01
Drift correction		0.03	0.03					
R_0 correction (added by CCT-K2)	0.12	0.063	0.038	0.024	0.007			
Type B combined uncertainty (mK)	0.22	0.28	0.28	0.17	0.20	0.16	0.13	0.07
Type A combined uncertainty (mK)	0.05	0.05	0.05	0.05	0.05	0.05	0.05	0.03
Standard combined uncertainty (mK)	0.23	0.29	0.28	0.18	0.21	0.17	0.14	0.08
Expanded uncertainty ($k=2$) (mK)	0.45	0.58	0.56	0.36	0.41	0.33	0.28	0.16

Table A.7: Uncertainty budget for PTB thermometers. A residual resistance correction was made to 1842381 during the comparison. These data (flagged with an asterisk, '*') do not represent the PTB realization of the ITS-90.

APPENDIX B

The complete bilateral equivalence matrices for each of the near-fixed-point comparison experiments are listed here. In these tables, the elements above the diagonal are the pair differences (row – column) expressed in mK, and the expanded ($k=2$) uncertainty of the pair difference (also in mK). This analysis represents the most complete and convenient summary of the experimental results, and forms the basis for the entry representing this Key Comparison into Appendix B of the MRA.

It is important to recall that only one NRC thermometer, serial number 1872174, was used in each of the two experimental comparisons. This provides an important link between the two data sets, and may be used in further analysis later on, outside the scope of this Report.

The elements below the diagonal in each of the Appendix B tables are $QDE_{0.95}$ confidence intervals [8] for the bilateral comparison (also expressed in mK). The $QDE_{0.95}$ value combines both the pair difference and the pair uncertainty into a single number, which represents the 95% confidence interval within which the two measurements can be expected to agree. This is a rigorous statistical approach to quantifying equivalence, which properly accounts for the joint probability given the two experimental probability distributions, and whose meaning and interpretation is explicit. In contrast, the "normalized difference" (sometimes called E_n) obtained by dividing the observed pair difference by the expanded ($k=2$) pair uncertainty is often difficult to interpret, and the "cutoff criterion" for "agreement" are not universally defined or applied. The utility of $QDE_{0.95}$ is not in the scientific evaluation of the metrology being performed here; rather, it is a simplified tool for end-users who wish to know the interval within which two laboratories can be expected to agree at a 95% level of confidence, based on the experiments reported here. It may have application within the context of evaluating the MRA Appendix C claims of the participants, for example. The simple formula for calculating $QDE_{0.95}$, given standard errors having normal distributions and infinite degrees of freedom is given in the following equation.

$$QDE_{0.95} \approx |\Delta| + \left\{ a + b \times \exp\left[\frac{-c|\Delta|}{u_p} \right] \right\} \times u_p$$

where $\Delta = m_2 - m_1$, a=1.654, b=0.3295, and c=4.05.

The last row and column in the bilateral equivalence matrices of Appendix B is the *KCRV*, which is treated as a "virtual laboratory" in order to generate the "equivalence to the Key Comparison Reference Value" information in a convenient fashion. Since all of the measurement uncertainty has been apportioned to the capsule temperatures, no uncertainty has been assigned to the *KCRV*. In practice, this amounts to saying that the *KCRV* is simply a constant evaluated statistically from this particular data set at each near-fixed-point temperature. The fact that the *KCRV* has no uncertainty associated with it in this comparison is an attempt to limit the likelihood of non-experts misinterpreting its meaning, beyond its intended application as a "baseline temperature for this comparison" which conveniently summarizes the work done in the Key Comparison.

	BNM	IMGC	NIST	NPL	NRC	KCRV
BNM	-	-2.39 ± 4.17	-3.13 ± 4.17	-2.78 ± 4.18	-2.45 ± 4.19	-2.71 ± 4.16
IMGC	*5.83*	-	-0.74 ± 0.47	-0.39 ± 0.53	-0.06 ± 0.56	-0.32 ± 0.32
NIST	*6.56*	*1.12*	-	0.35 ± 0.54	0.68 ± 0.57	0.42 ± 0.34
NPL	*6.22*	*0.82*	*0.79*	-	0.33 ± 0.62	0.07 ± 0.42
NRC	*5.90*	*0.56*	*1.15*	*0.84*	-	-0.26 ± 0.46
KCRV	*6.14*	*0.58*	*0.70*	*0.43*	*0.64*	-

	BNM	IMGC	NIST	NPL	NRC	PTB	KCRV
BNM	-	-2.43 ± 4.17	-3.02 ± 4.17	-2.55 ± 4.18	-2.33 ± 4.19	-2.58 ± 4.18	-2.60 ± 4.16
IMGC	*5.87*	-	-0.59 ± 0.47	-0.12 ± 0.48	0.10 ± 0.56	-0.15 ± 0.54	-0.17 ± 0.32
NIST	*6.45*	*0.97*	-	0.47 ± 0.50	0.69 ± 0.57	0.44 ± 0.56	0.42 ± 0.34
NPL	*5.99*	*0.53*	*0.88*	-	0.22 ± 0.58	-0.03 ± 0.57	-0.05 ± 0.36
NRC	*5.78*	*0.58*	*1.16*	*0.70*	-	-0.25 ± 0.64	-0.27 ± 0.46
PTB	*6.03*	*0.61*	*0.90*	*0.56*	*0.78*	-	-0.02 ± 0.44
KCRV	*6.03*	*0.43*	*0.70*	*0.37*	*0.65*	*0.43*	-

Table B.1 : Bilateral equivalence matrix for comparison measurements near the hydrogen triple point.

	NIST	NPL	NRC	KCRV
NIST	-	-0.07 ± 0.58	-0.06 ± 0.55	-0.01 ± 0.30
NPL	*0.59*	-	0.01 ± 0.68	0.06 ± 0.50
NRC	*0.55*	*0.67*	-	0.05 ± 0.46
KCRV	*0.29*	*0.50*	*0.46*	-

	NIST	NPL	NRC	PTB	KCRV
NIST	-	0.10 ± 0.55	-0.17 ± 0.55	-0.20 ± 0.67	0.01 ± 0.30
NPL	*0.57*	-	-0.27 ± 0.65	-0.30 ± 0.76	-0.09 ± 0.46
NRC	*0.63*	*0.81*	-	-0.03 ± 0.76	0.18 ± 0.46
PTB	*0.76*	*0.93*	*0.74*	-	0.21 ± 0.60
KCRV	*0.29*	*0.48*	*0.56*	*0.71*	-

Table B.2 : Bilateral equivalence matrix for comparison measurements near 17 K. Note that the NRC result at this temperature is derived from a calibration performed at NPL, and is not an independent realization.

	NIST	NPL	NRC	KCRV
NIST	-	0.06 ± 0.57	-0.06 ± 0.54	0.00 ± 0.28
NPL	*0.57*	-	-0.12 ± 0.68	-0.06 ± 0.50
NRC	*0.54*	*0.71*	-	0.06 ± 0.46
KCRV	*0.28*	*0.50*	*0.46*	-

	NIST	NPL	NRC	PTB	KCRV
NIST	-	-0.06 ± 0.54	-0.19 ± 0.54	-0.48 ± 0.66	-0.06 ± 0.28
NPL	*0.54*	-	-0.13 ± 0.65	-0.42 ± 0.76	0.00 ± 0.46
NRC	*0.64*	*0.69*	-	-0.29 ± 0.76	0.13 ± 0.46
PTB	*1.02*	*1.04*	*0.92*	-	0.42 ± 0.60
KCRV	*0.30*	*0.45*	*0.52*	*0.91*	-

Table B.3 : Bilateral equivalence matrix for comprison measurements near 20.3 K.

	BNM	IMGC	KRISS	NIST	NPL	NRC	KCRV
BNM	-	-0.13 ± 1.12	-0.03 ± 1.15	0.11 ± 1.13	0.08 ± 1.17	0.04 ± 1.17	-0.02 ± 1.08
IMGC	*1.12*	-	0.10 ± 0.49	0.24 ± 0.43	0.21 ± 0.52	0.17 ± 0.52	0.11 ± 0.28
KRISS	*1.13*	*0.52*	-	0.14 ± 0.51	0.11 ± 0.59	0.07 ± 0.59	0.01 ± 0.40
NIST	*1.12*	*0.59*	*0.57*	-	-0.03 ± 0.54	-0.07 ± 0.54	-0.13 ± 0.32
NPL	*1.15*	*0.64*	*0.62*	*0.53*	-	-0.04 ± 0.62	-0.10 ± 0.44
NRC	*1.14*	*0.61*	*0.60*	*0.55*	*0.61*	-	-0.06 ± 0.44
KCRV	*1.06*	*0.34*	*0.39*	*0.40*	*0.47*	*0.45*	-

	BNM	IMGC	KRISS	NIST	NPL	NRC	PTB	KCRV
BNM	-	-1.99 ± 2.81	-1.73 ± 2.83	-1.92 ± 2.82	-1.69 ± 2.83	-1.76 ± 2.83	-2.14 ± 2.83	-1.88 ± 2.80
IMGC	*4.31*	-	0.26 ± 0.49	0.07 ± 0.43	0.30 ± 0.47	0.23 ± 0.52	-0.15 ± 0.49	0.11 ± 0.28
KRISS	*4.06*	*0.66*	-	-0.19 ± 0.51	0.04 ± 0.55	-0.03 ± 0.59	-0.41 ± 0.57	-0.15 ± 0.40
NIST	*4.24*	*0.44*	*0.62*	-	0.23 ± 0.50	0.16 ± 0.54	-0.22 ± 0.51	0.04 ± 0.32
NPL	*4.02*	*0.69*	*0.54*	*0.64*	-	-0.07 ± 0.58	-0.45 ± 0.55	-0.19 ± 0.38
NRC	*4.09*	*0.66*	*0.58*	*0.62*	*0.58*	-	-0.38 ± 0.59	-0.12 ± 0.44
PTB	*4.47*	*0.56*	*0.88*	*0.64*	*0.90*	*0.87*	-	0.26 ± 0.40
KCRV	*4.19*	*0.34*	*0.48*	*0.32*	*0.50*	*0.49*	*0.59*	-

Table B.4 : Bilateral equivalence matrix for comparison measurements near the neon triple point.

	BNM	IMGC	KRISS	NIST	NPL	NRC	KCRV
BNM	-	0.13 ± 0.57	-0.16 ± 0.62	-0.14 ± 0.56	-0.09 ± 0.63	-0.25 ± 0.68	-0.07 ± 0.52
IMGC	0.62	-	-0.29 ± 0.42	-0.27 ± 0.31	-0.22 ± 0.43	-0.38 ± 0.50	-0.20 ± 0.24
KRISS	0.68	0.63	-	0.02 ± 0.39	0.07 ± 0.50	-0.09 ± 0.56	0.09 ± 0.34
NIST	0.61	0.53	0.39	-	0.05 ± 0.41	-0.11 ± 0.48	0.07 ± 0.20
NPL	0.64	0.58	0.50	0.41	-	-0.16 ± 0.57	0.02 ± 0.36
NRC	0.82	0.79	0.57	0.52	0.64	-	0.18 ± 0.44
KCRV	0.53	0.40	0.38	0.24	0.35	0.54	-

	BNM	IMGC	KRISS	NIST	NPL	NRC	PTB	KCRV
BNM	-	0.17 ± 0.55	-0.09 ± 0.60	0.06 ± 0.55	-0.05 ± 0.58	-0.23 ± 0.67	-0.17 ± 0.68	0.01 ± 0.50
IMGC	0.63	-	-0.26 ± 0.42	-0.11 ± 0.34	-0.22 ± 0.38	-0.40 ± 0.50	-0.34 ± 0.52	-0.16 ± 0.24
KRISS	0.62	0.60	-	0.15 ± 0.42	0.04 ± 0.45	-0.14 ± 0.56	-0.08 ± 0.57	0.10 ± 0.34
NIST	0.55	0.39	0.50	-	-0.11 ± 0.38	-0.29 ± 0.50	-0.23 ± 0.52	-0.05 ± 0.24
NPL	0.58	0.54	0.45	0.43	-	-0.18 ± 0.53	-0.12 ± 0.55	0.06 ± 0.30
NRC	0.78	0.81	0.61	0.70	0.62	-	0.06 ± 0.64	0.24 ± 0.44
PTB	0.74	0.77	0.58	0.66	0.59	0.63	-	0.18 ± 0.46
KCRV	0.49	0.36	0.38	0.25	0.32	0.60	0.56	-

Table B.5 : Bilateral equivalence matrix for comparison measurements near the oxygen triple point.

	BNM	IMGC	KRISS	NIST	NPL	NRC	KCRV
BNM	-	0.27 ± 0.45	-0.48 ± 0.52	0.07 ± 0.45	0.10 ± 0.52	-0.11 ± 0.59	0.07 ± 0.40
IMGC	0.64	-	-0.75 ± 0.39	-0.20 ± 0.28	-0.17 ± 0.39	-0.38 ± 0.48	-0.20 ± 0.20
KRISS	0.91	1.07	-	0.55 ± 0.39	0.58 ± 0.48	0.37 ± 0.56	0.55 ± 0.34
NIST	0.46	0.43	0.87	-	0.03 ± 0.39	-0.18 ± 0.48	0.00 ± 0.20
NPL	0.55	0.50	0.98	0.39	-	-0.21 ± 0.56	-0.03 ± 0.34
NRC	0.62	0.78	0.83	0.58	0.67	-	0.18 ± 0.44
KCRV	0.41	0.36	0.83	0.20	0.34	0.54	-

	BNM	IMGC	KRISS	NIST	NPL	NRC	PTB	KCRV
BNM	-	0.20 ± 0.48	0.10 ± 0.56	0.07 ± 0.49	0.15 ± 0.51	-0.13 ± 0.62	-0.11 ± 0.61	0.11 ± 0.44
IMGC	0.60	-	-0.10 ± 0.39	-0.13 ± 0.30	-0.05 ± 0.33	-0.33 ± 0.48	-0.31 ± 0.47	-0.09 ± 0.20
KRISS	0.58	0.43	-	-0.03 ± 0.40	0.05 ± 0.43	-0.23 ± 0.56	-0.21 ± 0.54	0.01 ± 0.34
NIST	0.50	0.38	0.40	-	0.08 ± 0.34	-0.20 ± 0.49	-0.18 ± 0.47	0.04 ± 0.22
NPL	0.58	0.34	0.43	0.37	-	-0.28 ± 0.51	-0.26 ± 0.49	-0.04 ± 0.26
NRC	0.66	0.73	0.69	0.61	0.70	-	0.02 ± 0.61	0.24 ± 0.44
PTB	0.63	0.69	0.66	0.57	0.67	0.60	-	0.22 ± 0.42
KCRV	0.48	0.26	0.33	0.23	0.27	0.60	0.57	-

Table B.6 : Bilateral equivalence matrix for comparison measruements near the argon triple point.

	BNM	IMGC	KRISS	NIST	NPL	NRC	KCRV
BNM	-	-0.17 ± 0.59	-0.11 ± 0.76	-0.35 ± 0.63	-0.34 ± 0.68	-0.09 ± 0.71	-0.23 ± 0.56
IMGC	*0.67*	-	0.06 ± 0.56	-0.18 ± 0.34	-0.17 ± 0.43	0.08 ± 0.48	-0.06 ± 0.20
KRISS	*0.78*	*0.56*	-	-0.24 ± 0.59	-0.23 ± 0.64	0.02 ± 0.68	-0.12 ± 0.52
NIST	*0.87*	*0.46*	*0.73*	-	0.01 ± 0.47	0.26 ± 0.52	0.12 ± 0.28
NPL	*0.90*	*0.53*	*0.77*	*0.46*	-	0.25 ± 0.58	0.11 ± 0.38
NRC	*0.72*	*0.50*	*0.67*	*0.69*	*0.73*	-	-0.14 ± 0.44
KCRV	*0.69*	*0.23*	*0.56*	*0.35*	*0.43*	*0.51*	-

	BNM	IMGC	KRISS	NIST	NPL	NRC	PTB	KCRV
BNM	-	-0.80 ± 0.59	-1.10 ± 0.76	-0.96 ± 0.61	-0.85 ± 0.66	-0.73 ± 0.71	-0.93 ± 0.68	-0.87 ± 0.56
IMGC	*1.29*	-	-0.30 ± 0.56	-0.16 ± 0.31	-0.05 ± 0.39	0.07 ± 0.48	-0.13 ± 0.43	-0.07 ± 0.20
KRISS	*1.73*	*0.76*	-	0.14 ± 0.57	0.25 ± 0.62	0.37 ± 0.68	0.17 ± 0.64	0.23 ± 0.52
NIST	*1.46*	*0.42*	*0.62*	-	0.11 ± 0.42	0.23 ± 0.50	0.03 ± 0.45	0.09 ± 0.24
NPL	*1.39*	*0.40*	*0.76*	*0.46*	-	0.12 ± 0.56	-0.08 ± 0.51	-0.02 ± 0.34
NRC	*1.32*	*0.49*	*0.93*	*0.64*	*0.59*	-	-0.20 ± 0.58	-0.14 ± 0.44
PTB	*1.49*	*0.49*	*0.71*	*0.44*	*0.52*	*0.68*	-	0.06 ± 0.38
KCRV	*1.33*	*0.24*	*0.66*	*0.29*	*0.33*	*0.51*	*0.39*	-

Table B.7 : Bilateral equivalence matrix for comparison measurements near the mercury triple point.